Environmental Science & Technology

pubs.acs.org/est

Article

Disposition of Fluorine on New Firefighter Turnout Gear

Derek J. Muensterman, Ivan A. Titaley, Graham F. Peaslee, Leah D. Minc, Liliana Cahuas, Alix E. Rodowa, Yuki Horiuchi, Shogo Yamane, Thierry N.J. Fouquet, John C. Kissel, Courtney C. Carignan, and Jennifer A. Field*

Cite This: *Environ. Sci. Technol.* 2022, 56, 974−983

Read Online

ACCESS | Metrics & More | Article Recommendations | Supporting Information

ABSTRACT: Firefighter turnout gear is essential for reducing occupational exposure to hazardous chemicals during training and fire events. Per-and polyfluoroalkyl substances (PFASs) are observed in firefighter serum, and possible occupational sources include the air and dust of fires, aqueous film-forming foam, and turnout gear. Limited data exist for nonvolatile and volatile PFASs on firefighter turnout gear and the disposition of fluorine on the individual layers of turnout gear. Further implications for exposure to fluorine on turnout gear are not well understood. Three unused turnout garments purchased in 2019 and one purchased in 2008, were analyzed for 50 nonvolatile and 15 volatile PFASs by liquid chromatography quadrupole time-of-flight mass spectrometry (LC-qTOF-MS) and gas chromatography−mass spectrometry (GC−MS), respectively. Particle-induced gamma ray emission (PIGE), a surface technique, and instrumental neutron activation analysis (INAA), a bulk technique, were used to measure total fluorine. Bulk characterization of the layers by pyrolysis-GC/MS (py-GC/MS) was used to differentiate fluoropolymer (e.g., PTFE) films from textile layers finished with side-chain polymers. The outer layer, moisture barrier, and thermal layers of the turnout gear all yielded measured concentrations of volatile PFASs that exceeded nonvolatile PFAS concentrations, but the summed molar concentrations made up only a small fraction of total fluorine (0.0016−6.7%). Moisture barrier layers comprised a PTFE film, as determined by py-GC−MS, and gave the highest individual nonvolatile (0.159 mg F/kg) and volatile PFAS (20.7 mg F/kg) as well as total fluorine (122,000 mg F/kg) concentrations. Outer and thermal layers comprised aromatic polyamide-based fibers (aramid) treated with side-chain fluoropolymers and had lower levels of individual nonvolatile and volatile PFASs. Equal concentrations of total fluorine by both PIGE and INAA on the outer and thermal layers is consistent with treatment with a side-chain fluoropolymer coating. New turnout gear should be examined as a potential source of firefighter occupational exposure to nonvolatile and volatile PFASs in future assessments.

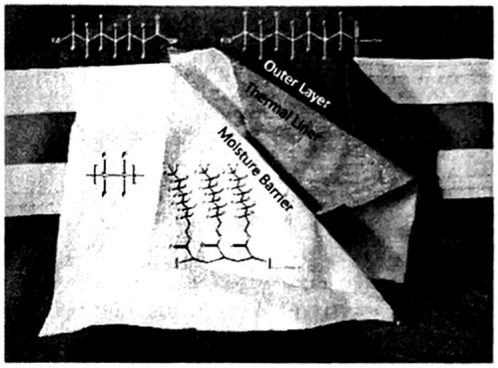

KEYWORDS: *firefighter turnout gear, side-chain fluoropolymer, PFAS, total fluorine, PTFE, meta- and para-aramid, pyrolysis-GC/MS*

■ INTRODUCTION

Occupational exposure to harmful chemicals in the firefighting industry is an increasing concern among firefighters. Chemicals of concern include polycyclic aromatic hydrocarbons,[1] metals,[1] formaldehyde,[2] 1,3-butadiene,[3] and per- and polyfluoroalkyl substances (PFASs).[4−7] Elevated concentrations of PFASs are found in dust from fire stations[8,9] and are detected in firefighter serum.[6,10−13] Laitinen et al. suggested that used personal protective equipment (e.g., turnout gear) contaminated by aqueous film-forming foam as a possible source of firefighter exposure to PFASs,[4] but exposure to PFASs imbedded in the turnout gear during manufacturing has not been examined. Another concern is the end-of-life treatment of turnout garments, as Chen et al. have extensively studied the disposal phase of PFAS-treated carpets and have suggested that PFASs could leach into the environment directly through air emissions or leachates in unlined landfills.[14] Alternatively, leaching of PFASs into the environment could occur indirectly by wastewater treatment plants in line landfills.[14]

Turnout gear is personal protective equipment worn by firefighters to minimize occupational exposure to hazardous conditions (heat, chemicals, radiation, etc.) during fire and training events. Turnout gear are complex, multilayer garments designed for performance under extreme thermal conditions. The outer (OU) layer provides resistance to heat, oil, and water and serves as an exoskeleton for the underlying layers. The moisture barrier (MB) layer is typically manufactured with the fluoropolymer polytetrafluoroethylene (PTFE) in order to

Received: September 21, 2021
Revised: December 14, 2021
Accepted: December 15, 2021
Published: December 27, 2021

https://doi.org/10.1021/acs.est.1c06322
Environ. Sci. Technol. 2022, 56, 974−983

obtain a desired water repellency. The thermal (TL) layer wicks moisture and is the closest to the skin.

New (unused) turnout gear has measurable PFASs. For example, Rewerts et al. found 6:2−10:2 fluorotelomer alcohols (FTOHs) on a single newly manufactured firefighter jacket,[15] while Shinde and Ormond reported the tentative identification of 10:2 FTOH in the OU and MB layers of one turnout gear garment.[16] Peaslee et al.[17] reported nonvolatile PFASs for individual layers in new firefighter turnout gear after base-assisted extraction. To date, there are no systematic measurements of volatile PFASs, nor have the layers of turnout gear been characterized for their bulk chemical composition (e.g., fluoropolymer films).

Peaslee et al.[17] also reported total fluorine by particle-induced gamma ray emission (PIGE), but the PIGE signals were off scale and thus total fluorine could not be quantified on the MB layer. Therefore, methods with a greater linear range, such as instrumental neutron activation analysis (INAA),[32,33] are needed to quantify very high levels of total fluorine. To date, INAA is used to quantify trace-elements in textile dyes.[18,19] The combination of PIGE and INAA can more completely describe the nature and location (e.g., disposition) of fluorine on turnout gear layers, since PIGE quantifies fluorine in the top 150−220 μm of textiles[20] and INAA interrogates the entire depth of the material.

We also propose a method to characterize the presence of fluoropolymer films in textiles. To the best of our knowledge, no attempts have been made to analytically distinguish between textile layers comprising fluoropolymer films (e.g., polytetrafluoroethene or PTFE) from textile layers treated by industrial processes such as the application of side-chain fluoropolymers using a water-based fluoropolymer emulsion process.[21] Pyrolysis-gas chromatography−mass spectrometry (py-GC/MS) is a conventional technique for the bulk characterization of polymers (e.g., synthetic) and natural fibers.[22,23] Volatile compounds are generated by pyrolysis and analyzed by mass spectrometry, resulting in reproducible fingerprints[24,25] that are visually compared to fingerprints in the literature or databases (e.g. NIST database) to infer the chemical nature of the polymer.[26] Matches are ranked by the similarity of mass spectral data (e.g., similarity indices or spectral contrast angles).[27] While pyrolysis products are tentatively assigned by this process, the overall polymer family cannot be identified. Newer algorithms rely on automatic comparison of py-GC/MS data with predefined peak lists generated from standards that are archetypical of a known polymer class.[28] Similarity indices are obtained from correlation coefficients.[27] To gain deeper insight into the chemistry of the textile sublayers, fluoropolymer (e.g., PTFE) films were differentiated from textile layers treated with side-chain fluoropolymers[21] using py-GC/MS. Data analysis consisted of a set of mass spectra from the py-GC/MS profiles from samples and/or standards, which eliminates the need for a predefined list of characteristic peaks and correlation coefficients.

It is important to understand the disposition (e.g., location and arrangement) of fluorine when considering the firefighter exposure to PFASs, since the bioavailability and toxicity of fluoropolymers, side-chain fluoropolymers, and individual PFASs depend on their material properties and chemical structure. Although fluoropolymers were categorized as "polymers of low concern",[29] Lohmann et al.[30] indicated that it is premature to discount the potential for fluoropolymers (e.g., PTFE) to penetrate cell membranes based solely on their size. Side-chain fluoropolymers degrade slowly under environmental conditions, releasing individual PFASs.[31−33] However, laundering,[34] weathering,[35] and the heat of fires may accelerate side-chain fluoropolymer degradation and, thus, exposure to individual PFASs. As for individual PFASs, they are bioavailable through water and diet, and US health advisory levels are available for PFOS and PFOA and many states have health advisory levels for other nonvolatile PFASs.[36]

The objective of this study was to characterize the chemical composition, including individual PFASs, total fluorine, and polymers of the individual layers of three newly manufactured unused turnout garments purchased in 2019 and one unused garment purchased in 2008. For individual PFASs, 50 target nonvolatile and 15 target volatile PFASs were determined by liquid chromatography quadrupole time-of-flight mass spectrometry (LC-qTOF-MS) and gas chromatography−mass spectrometry (GC−MS), respectively. Total fluorine was measured by PIGE and INAA and used together with the bulk characterization of individual sublayers by py-GC/MS. A solution relying on the systematic evaluation of spectral contrast-angles[37] is also proposed for polymer identification by py-GC/MS.

■ EXPERIMENTAL METHODS

Standards and Reagents. Chemical and reagent source, purity, and acronyms for the 50 target nonvolatile PFASs, including perfluorocarboxylates (C4−C14 and C16); perfluorosulfonates (C3−10); Cl-PFOS; cyclic sulfonates (PFEtCHxS); substituted sulfonamides (MeFOSA and EtFOSA); sulfonamide acetic acids (FOSAA, MeFOSAA, and EtFOSAA); x:2 telomer sulfonates (C4, 6, 8, and 10); saturated telomer acids x:2 (C6, 8, and 10); unsaturated telomer acids x:2 (C6 and 8); hexafluoropropylene oxide dimer acid (HFPO-DA); dodecafluoro-3*H*-4,8-dioxanoate (ADONA); 9-chlorohexadecafluoro-3-oxanonane-1-sulfonate and 11-chloroeicosafluoro-3-oxaundecane-1-sulfonate (9Cl-PF3ONS and11l-PF3OUdS); bis(1*H*,1*H*,2*H*,2*H*-perfluorooctyl)phosphate and bis(1*H*,1*H*,2*H*,2*H*-perfluorodecyl)phosphate (6:2diPAP and 8:2diPAP); and bis-[2-(*N*-ethyleperflurooctane-1-sulfonamido)ethyl] phosphate (diSAmPAP) were purchased from Wellington Laboratories (Guelph, ON, Canada) and are listed in the Supporting Information (SI) (Table S1). In addition, 31 mass-labeled surrogate standards and two mass-labeled internal (instrumental) standards of PFOA and PFOS were used for quantification (Table S1).

Chemical source, purity, and acronyms for the 15 target volatile PFASs, including 4:2−10:2 fluorotelomer alcohols (FTOHs), *N*-methyl and -ethyl perfluooctanesulfonamides (MeFOSA and EtFOSA, respectively), *N*-methyl and -ethyl perfluorooctane sulfonamido ethanols (MeFOSE and EtFOSE, respectively), 8:2−10:2 fluorotelomer acrylates (FTAcs) purchased from Wellington Laboratories (Guelph, ON, Canada), and 12:2 FTOH, 4:2−6:2 FTAcs, and 6:2−8:2 fluorotelomer methylacrylates (FTMAcs) purchased from SynQuest Laboratories (Alachua, FL) are listed in the SI (Table S2). Ten mass-labeled internal standards (4:2, 6:2, 8:2, 10:2 FTOH, Et- and MeFOSA, and Me- and EtFOSE purchased from Wellington Laboratories (Guelph, ON, Canada), and 6:2 FTAc and 6:2 FTMAc purchased from Sapphire North America (Ann Arbor, MI)) were used to quantify the target analytes. A total of 24 additional suspect

https://doi.org/10.1021/acs.est.1c06322

Table 1. Firefighter Turnout Gear Suite Number (Year of Manufacture), Including Thermal Liner (TL), Moisture Barrier (MB), and Outer (OU) Layers, Total Nonvolatile and Volatile PFASs, Total Fluorine by either [1]PIGE or [2]INAA, and Bulk Polymer Characterization of Sublayers by Py-GC/MS

	layer	nonvolatile PFAS (mg F/kg)	volatile PFAS (mg F/kg)	total fluorine (mg F/kg)	individual sublayers characterized by py-GC/MS
FF1 (2019)	TL[a]	0.00433	0.00827	18[1]	unknown aramid[g]
					unknown aramid[g]
					unknown aramid[g]
	MB[a]	0.119	20.7	122,000[2]	*PTFE*
					meta-aramid
	OU[a,b]	0.0838 ± 0.117	0.899 ± 0.0911	4950[2]	unknown aramid[g]
					para-aramid
FF2 (2019)	TL[a,c]	0.0220	0.606	1430[2]	unknown aramid[g]
					unknown aramid[g]
					unknown aramid[g]
	MB[a,c]	0.159	18.8	120,000[2]	*PTFE*
					meta-aramid
	OU[b,d]	0.0247	0.340	2650[2]	unknown aramid[g]
					para-aramid
FF3 (2008)	TL[c]	0.0453	0.825	13[2]	unknown aramid[g]
					unknown aramid[g]
					unknown aramid[g]
	MB[c]	0.0569	4.33	116,000[2]	*PTFE*
					meta-aramid
	OU[c,b]	0.0218	3.26	2360[2]	para-aramid
FF4 (2019)	TL[a]	0.0248	0.233	17[1]	unknown aramid[g]
					unknown aramid[g]
					unknown aramid[g]
	MB[a,c]	0.0438	0.671	43,700[2]	*PTFE*
					meta-aramid
	OU[b,f]	0.00993	10.9	5480[2]	unknown aramid[g]
					para-aramid

[a]Meta-aramid. [b]Para-aramid. [c]PTFE. [d]Polybenzimidazole. [e]No information available. [f]High-density carbon shell. [g]Unknown aramid fiber.

compounds were analyzed including 14:2 FTOH, C3−C7 methyl perfluoroalkane sulfonamido ethanols (MeFASEs), C2−C7 ethyl perfluoroalkane sulfonamido ethanols (EtFASEs), 4:2−10:2 fluorotelomer iodides (FTIs), C4, C6, C8, and C10 perfluoroalkyl iodides (PFIs), and 6:2−12:2 fluorotelomer olefins (FTOs) (Table S3). Pyrolysis-GC/MS utilized a PTFE standard (Scientific polymer Products Inc., Ontario, NY) and purchased samples of poly(*N*,*N*-(1,3-phenylene)isophthalamide) (Nomex, meta-aramid) and para phenylene terephthalamide (Kevlar, para-aramid) from Sigma-Aldrich, St Louis, MO.

Firefighter Turnout Gear. Four unused firefighter turnout pants were donated by the International Association of Fire Fighters (IAFF) and each was made by a different manufacturer (labeled in this study as FF1−FF4). Some information on the fabric composition was publicly available (Table 1). Manufacturing dates of the turnout pants were 2008 (one garment) and 2019 (three garments) (Table 1). Each garment was separated into OU, MB, and TL layers and then cut into 2 × 2 cm^2 and 1.5 × 1.5 cm^2 pieces using methanol-rinsed scissors for LC-qTOF and GC−MS analysis, respectively.

Extraction and Analysis of Nonvolatiles by LC-qTOF. Masses of each sample had a target weight of 0.30 (±0.01) g; 0.9 ng of each mass-labeled surrogate was spiked into all 15 mL polypropylene tubes prior to extraction and samples were subject to methanol extraction as adapted from Robel et al.[38] Adaptations included the addition of an extracted internal standard and a concentration step. After the final 10 mL of extract is reached, 30 μL of ethylene glycol is added to each centrifuge tube and samples were concentrated under nitrogen to a final volume of 150 μL. Analysis consisted of a 50 μL aliquot of each extract into 150 μL conical vials and 0.30 ng of each mass-labeled internal standard was used to calculate recovery of the extracted mass-labeled surrogate. The separation and detection of nonvolatile PFASs were performed by liquid chromatography (Agilent 1260 HPLC) with a SCIEX 5500 qTOF interface with an electrospray ionization source that was operated in a negative-ion mode as previously described.[39] The gradient for both mobile phases is described in detail by Backe et al.,[40] while target PFAS identification and quantification are described by Schwichtenberg et al.[39] See the SI for additional details on whole method accuracy, precision, and LOD/LOQ (Tables S4 and S5). To compute total fluorine from individual PFAS concentrations, values that were <LOD or <LOQ were replaced with either 0 (for a minimum estimate) and for the maximum estimate, values <LOD were replaced with the measured LOD (Tables S4 and S6) and values <LOQ were replaced with the measured LOQ (Tables S4 and S6).

Extraction and Analysis of Volatiles by GC−MS. Masses of samples ranged from 0.035 to 0.070 g and were subjected to a methanol extraction, as modified from Rewerts et al.[15] Samples were placed in 1.5 mL GC vials with methanol, spiked with internal standards, sonicated for 30 min at 25 °C, and then directly analyzed without any further cleanup. Analyses were performed by concurrent, solvent recondensation, large-volume splitless injection coupled with mass

https://doi.org/10.1021/acs.est.1c06322
Environ. Sci. Technol. 2022, 56, 974−983

spectrometry. Extracts (10 μL) were injected in splitless mode with an inlet temperature of 280 °C. Separations were performed using an Agilent deactivated, fused silica tubing capillary column (5 m × 0.53 mm i.d.) connected to a Restek Rxi-624Sil MS capillary column (30 m × 0.25 mm i.d., 1.40 μm film thickness). Further description of GC parameters is provided in the SI along with additional details on whole method accuracy, precision, and LOD/LOQ (Table S6).

Total Fluorine Analysis by PIGE. Sample preparation for textiles was performed for PIGE as described in Ritter et al.[41] Briefly, using methanol-rinsed scissors, 2 × 2 cm^2 areas were cut from each layer of the firefighter turnout gear. Samples were mounted using clear adhesive tape onto a stainless-steel target frame with a 1 cm diameter hole for the ex vacuo ion beam analysis. Only one side from each layer was interrogated. For example, in the OU and TL layers, the exterior-facing sides were subject to the ion beam, whereas the inner-facing side of the MB was exposed to the ion beam. Total fluorine in ppm was determined from an external calibration curve using sodium fluoride standards prepared in cellulose nitrate mixtures. The concentration was converted into nmol F/cm^2 based on the density of each sample. For each measurement, the total fluorine concentration measured by gamma rays was normalized to Ar gamma rays in the atmosphere.[42] The calculated accuracy and precision does not apply to the MB layers due to the presence of PTFE in the layers, which resulted in total fluorine concentrations exceeding the calibration curve for PIGE analysis (>100,000 mg F/kg). Further discussion on the difficulty to measure total F in MB layers and conversion to nmol F/cm^2 are provided in the SI.

Total Fluorine Analysis by INAA. To further characterize total fluorine content, this study utilized the thermal neutron reaction $^{19}F(n,\gamma)^{20}F$ where the resultant product decays with a half-life of 11.03 s and emits a characteristic gamma ray at 1633.6 keV. Firefighter turnout gear samples were encapsulated in high density polyethylene (HDPE) NAA grade 2 dram vials (LA Plastics, Yorba Linda, CA) and weighed to the nearest 0.1 mg, with sample masses ranging from ca. 150−2000 mg, depending on anticipated F concentrations. Three replicates of CaF_2 (99.5%, Alfa Aesar, Haverhill, MA) were similarly encapsulated, with masses of ca. 25 mg each. Samples and standards were irradiated for 40 s at a thermal neutron flux of 10^{13} n·(cm^{-2}·s^{-1}), using the pneumatic tube facility at Oregon State University and then counted for 60 s using a 26% relative efficiency high purity germanium detector (ORTEC, Oak Ridge, TN) at a distance of 5 cm from the detector face. Sample quantification in ppm was based on the responses of the CaF_2 standards, using the weighted mean to convert activity to mass, and was converted to nmol F/cm^2. Additional details on whole method accuracy, precision, and LOD/LOQ are provided the SI.

Bulk Characterization by Py-GC/MS. The three layers of each firefighter turnout gear were manually separated into their individual respective sublayers (e.g., black film and white fabric and brown/black threads, Table S7). Separation of the three layers resulted in a total of 27 sublayers. The py-GC/MS workflow is depicted in Figure S1. Pyrolysis-GC/MS experiments were conducted using an EGA/PY-3030 pyrolyzer (Frontier Lab., Japan) and an Agilent 7890B GC with an Agilent HP-5 capillary column (30 m × 0.25 mm, 0.15 μm film thickness). Pyrolysis-GC/MS profiles composed of 3480 scans were exported as netCDF files using the proprietary program msAxel (JEOL, Japan), which was also used for the control of the instrument. The netCDF files were imported to the freeware Kendo (AIST, Japan) written with Visual Studio (Microsoft, USA) for the processing and visualization of mass spectral data.[43,44] All the files were first thresholded at 1000 counts (average background signal from the detector before the py-GC/MS analysis) and "CF_2-filtered" scan-by-scan to extract any peak series spaced by 49.9968 (mass of a CF_2 moiety) ±0.003 Da, which was the tolerance chosen based on the dispersion of m/z values for the peak from hexamethylcyclotrisiloxane at m/z 207.0324 over 10 min of analysis.

The similarity of the extracted profiles compared with the py-GC/MS profile of a PTFE was evaluated by systematically computing a spectral contrast angle "theta"[37] between the mass spectra integrated over three scans for samples and the PTFE standard, which resulted in 1160 angles computed in total. The spectral contrast angle θ corresponds to the angle between the two mass spectra seen as vectors. The θ angle of two mass spectra with a similar peak list and similar relative abundance peak to peak tends to 0. Mass spectra with a θ angle $\leq 5^0$ were considered identical in the present study. The quantification of the degree of similarity/dissimilarity was then conducted using the spectral contrast angle method[37] for the summed mass spectra from three scans at a time for the FF sample and the PTFE standard (see the SI for more details). Consecutive sets of three scans and their summed mass spectra with a θ angle $<5^0$ were further combined to get a reduced list of matching GC peaks between the FF sample and PTFE with no need for a predefined list of characteristic peaks. The same procedure was applied for the comparison of the remainder of py-GC/MS profiles after CF_2-filtering with a meta-aramid standard.

■ RESULTS AND DISCUSSION

Target Nonvolatile PFASs. A total of 24 target individual nonvolatile PFASs from four classes were quantified on one or more firefighter turnout gear layers (Tables S8−S11). All three layers of the four turnout pants gave extensive perfluorocaraboxylic acid (PFCA) homolog series, typically ranging from C4 up to C14, with C4−C10 as the most abundant (Table S8). The most frequently detected (100%) were PFBA (C4), PFHxA (C6), and PFHpA (C7) (Table S8 and Figure S2). While PFOS was detected in 11/12 layers, other perfluorosulfonic acids (PFSAs) (Table S9) and ECF- and fluorotelomer-derived PFASs were only infrequently detected (Tables S10 and S11). Exceptions included 6:2 FtS (5/12 layers), 6:2 diPAP (7/12 layers), and diSamPAP (4/12 layers) (Table S11). Total concentrations of nonvolatile PFASs were greatest in the MB, followed by TL and OU layers (Table 1). Concentrations for PFASs on textiles are reported in units of μg/m^2[15,35,38,45] and ng/g[17,46,47] because a subset of prior literature reports these units for textiles. To convert from units of μg/m^2 to ng/g, the densities of each layer are provided in Table S8 along with an equation to convert between units (eq S4).

Peaslee et al. reported PFCA homolog series in firefighter turnout gear but at much higher concentrations (e.g., 805 ng/g PFOA).[17] In contrast, the highest reported PFCA in the present study was for PFDoA in FF2-MB (61 ng/g; Table S8) and was comparable to PFCA concentrations for other types of durable water-repellent clothing.[35] Durable water repellent clothing consists of outdoor jackets, skiwear, fisherman's garments, military garments, and chemical production protective garments. The basic methanol extraction conditions employed by Peaslee et al. most likely have resulted in higher

https://doi.org/10.1021/acs.est.1c06322
Environ. Sci. Technol. 2022, 56, 974−983

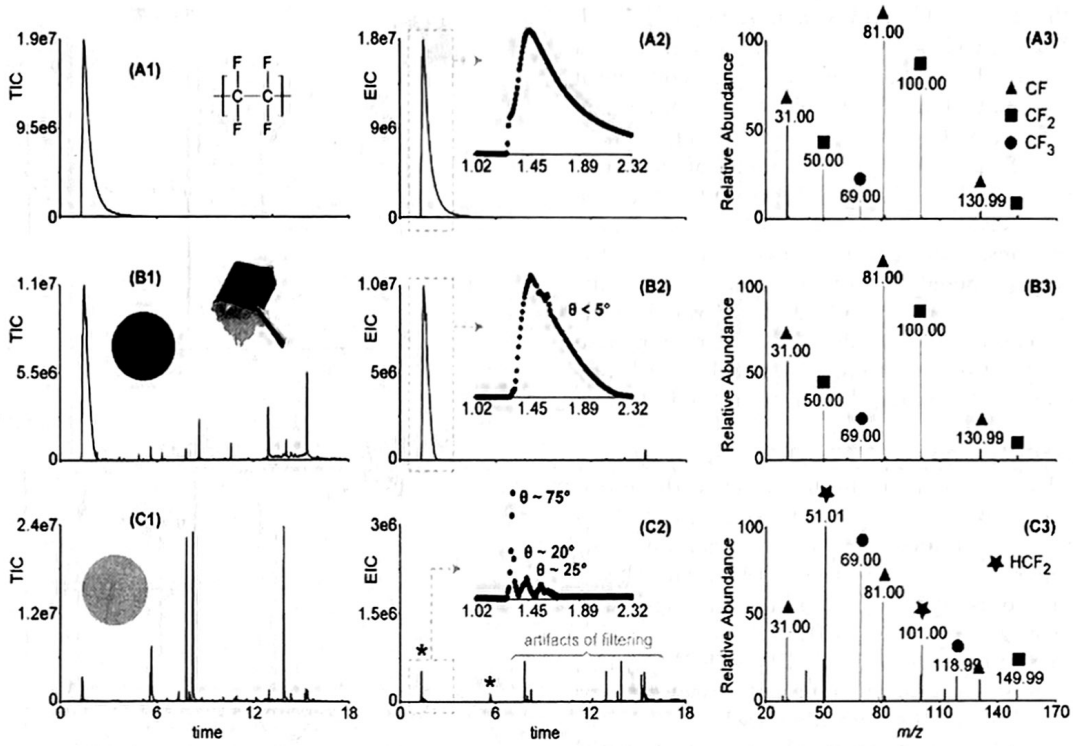

Figure 1. Py-GC/MS chromatograms (A1), after filtering for $-(CF)_2$ series (A2), and the sum the mass spectrum for the PTFE standard (A3); the black sublayer of the MB for FF1 (B1−B3); and the white sublayer of the MF of FF1 (C1−C3). Insets in A2 and B2 show magnification of the py-GC/MS profiles (1.02−2.32 min). Red dots indicate scans with a spectral contrast angle $\theta < 5°$, which indicates a high similarity with the PTFE standard.

observed PFCA and PFSA concentrations. Methanol is recognized as not being exhaustive in the extraction of individual PFASs from side-chain fluoropolymers.[33,48] Solvents such as tetrahydrofuran or methyl *tert*-butyl ether are more appropriate for exhaustive extraction of side-chain fluoropolymers. However, as a weaker extraction solvent, methanol may preferentially extract loosely bound, and potentially more bioavailable PFASs from the surfaces of polymers and materials coated in side-chain fluoropolymers.

Target Volatile PFASs. Nine target volatile PFASs including 6:2, 8:2, 10:2, and 12:2 FTOH, Me- and Et-FOSE, 8:2 and 10:2 FTAc, and 6:2 FTMAc were quantified in at least one turnout gear layer (Tables S12 and S13). The total concentrations of volatile PFASs were higher than the nonvolatile PFASs in all layers (Table 1), and concentrations were the greatest in the MB, followed by OU and TL layers (Table 1). Longer-chain FTOHs including 8:2, 10:2, and 12:2 FTOH and Me- and Et-FOSE were only measured in FF3, which was an older suit from 2008 when C8 chemistry was still in use (Tables S12 and S13). Pants from 2019 (FF-1,2, and 4) only gave 6:2 FTOH (Table S12), which may reflect the change from C8 to C6-based PFAS chemistry.[49] In addition, 6:2 FTMAc, which is a side-chain polymer intermediate,[50,51] was found at the highest frequency (100%). The 8:2 and 10:2 FTAc were in FF4, which indicates the use of long-chain chemistry, despite FF-4 being manufactured in 2019 (Table S13). Deng et al. previously demonstrated the use of 6:2 FTMAc to impart superhydrophobicity to fabric.[52] van der Veen et al. also reported 6:2 FTMAc and 6:2−10:2 FTOHs on other types of durable water-repellent clothing.[35]

Of the 24 volatile suspects, only MeFBSE was detected in only FF1- and FF2-MB (Table S12). The identity of MeFBSE was confirmed from injection of a mixture of standards provided by 3M. MeFBSE was first reported in a 1988 upholstery material[15] but the identity was not confirmed. The chemical is structurally similar to a chemical released from a manufacturing plant in Alabama,[53] [(*N*,*N*-bis(2-hydroxyethyl)]perfluorobutanesulfonamide (FBSEE), which is an intermediate in PFAS production. There are currently no known toxicity data for MeFBSE, though 3M announced it would conduct toxicity analysis of FBSEE and FBSE.[54] The extracts were analyzed in full scan PCI mode to determine the presence of any secondary FTOHs (sFTOHs),[31] but none were detected.

Total Fluorine. Both PIGE and INAA gave high total fluorine in all four MB layers (Table S14). However, PIGE values for the MBs were off scale (>100,000 mg F/kg), while INAA gave values ranging from 43,700 to 122,000 mg F/kg (Table 1). Total fluorine by PIGE for MBs was not reported by Peaslee et al. since the levels were too high[17] and were attributed to the fluoropolymer (e.g., PTFE).

All four OU layers gave the next highest levels of total fluorine (Tables 1 and S14), but were a factor of 10 lower than those reported by Peaslee et al.[17] However, total fluorine for the OU layers were similar to that of Schellenberger et al. who used a padding process to apply side-chain fluoropolymers to textiles.[34] Of three turnout gear layers, TL layers gave the lowest levels of total fluorine (Tables 1 and S14). The TL layers from FF1, FF3, and FF4 (Table 1) had <LOD or lower (e.g., ≤32 mg F/kg) fluorine levels by either total fluorine technique (Table S14). The total fluorine of FF2-TL was in the same order of magnitude of the total fluorine in FF2-OU, which indicates that the TL layer of FF2 was likely treated with fluorine. Publicly available information indicated that FF2-TL

https://doi.org/10.1021/acs.est.1c06322
Environ. Sci. Technol. 2022, 56, 974−983

was treated with PTFE (Table 1). Visual inspection of FF2-TL sublayers following py-GC/MS analysis did not indicate a PTFE sublayer, but indicated the presence of a different type of fluorinated treatment. Low levels of total fluorine and individual nonvolatile and volatile PFASs on the TL layers in FF1, 3, and 4 are unlikely to be the result of deliberate treatment to impart water and oil repellency and may be the result of processing textile within a facility that regularly applies fluorinated coatings. Alternatively, migration of PFASs between layers is proposed by Peaslee et al.[17] Overall, the summed molar concentrations of individual PFASs only made up a small fraction of total fluorine where minimum contributions ranged from 0.0016 to 6.3% (Table 1), whereas the maximum contributions ranged from 0.0018 to 6.4% (data not shown).

Bulk Characterization by Py-GC/MS. The py-GC/MS profile of a PTFE standard displayed an early broad chromatographic peak (Figure 1A1), which, when "CF_2-filtered", gave a simpler total ion chromatogram with only the early eluting peak remaining (Figure 1A2). The filtered chromatographic peak gave an associated average mass spectrum displaying $(CF_2)nCF^{+\bullet}$ (31, 81, and 131 m/z), $(CF_2)n^{+\bullet}$ (50, 100, and 150 m/z), and $(CF_2)nCF_3^{+\bullet}$ (69, 119, and 169 m/z) ion series archetypical of perfluorinated chains (Figure 1A3).[22] All four MBs were comprised of two layers, one of which gave a broad chromatographic peak as illustrated by the black sublayer of FF1-MB (Figure 1B1). When this sublayer was "CF_2-filtered", a single chromatographic peak was obtained (Figure 1B2), which matched with the chromatogram of the PTFE standard (Figure 1A1,A2). Similarly, the comparison of the average mass spectrum of the black sublayer of FF1-MB (Figure 1B3) matched with that of the PTFE standard (Figure 1A3). Therefore, the py-GC/MS analysis confirmed the presence of the PTFE sublayer in the MB layers, as suggested by publicly available information (Table 1) and the high amount of total fluorine observed in this study (Tables 1 and S14) and in the previous study by Peaslee et al.[17]

While the black sublayer closely matched the PTFE profile, the white sublayer of the FF1-MB layer (Figure 1C1) did not give an early chromatographic peak (Figure 1C2) that was characteristic of the PTFE standard (Figure 1A1). The CF_2-filtered chromatogram only showed very small peaks (Figure 1C2 and inset) and the spectral contrast angle was greater than 20%. However, this sublayer showed a high similarity for six major GC peaks of the meta-aramid standard with spectral contrast angles $\theta < 5°$ (Figure 2A1,A2) for their corresponding mass spectra. The meta-aramid standard did not show evidence of fluorine, which was consistent with the chemical structure of meta-aramid (Figure 2A2).

Analyses by py-GC–MS of TL and OU layers gave a poor match with PTFE and meta-aramid but gave high similarities with a para-aramid standard with seven major GC peaks and spectral contrast angles $\theta < 5°$ (Figure 2B1,B2 and Figure S8) for four of the seven of the TL sublayers. The para-aramid standard did not show evidence of fluorine but was consistent with the chemical structure of para-aramid (Figure 2B2). Three of the seven TL and all OU sublayers did not have a good match with either meta- or para-aramid (Figure S10A,B) and was attributed to an unknown type of aramid (Table 1). In addition to confirmation of meta- and para-aramid profiles, extraction of –(CF2)n– series from the py-GC/MS chromatograms of the OU (Figures S7 and S8) and TL sublayers

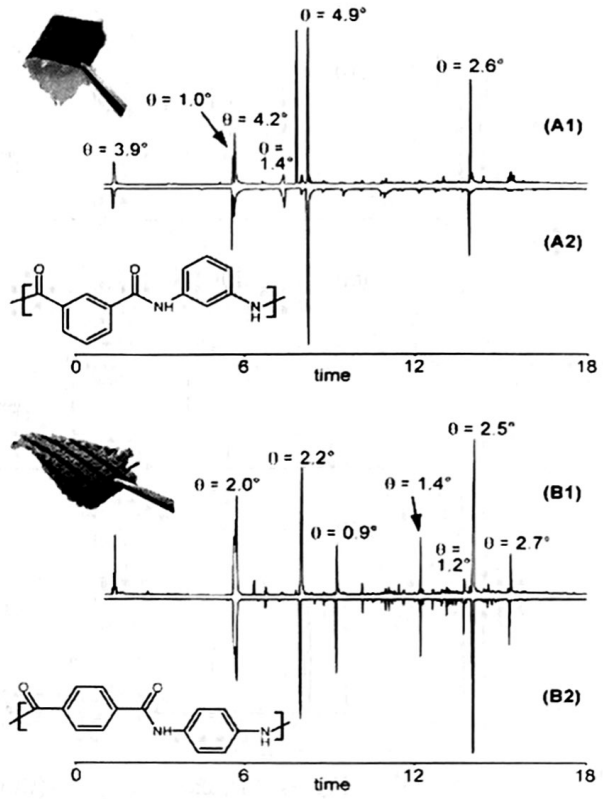

Figure 2. Py-GC/MS total ion chromatogram of the FF1-MB white fabric (black line) (A1) with the TIC profile of the meta-aramid standard (A2) and the FF1-OU black yarn (B1) with the TIC profile of the para-aramid standard (B2) with their respective spectral contrast angles, θ, which refers to the mass spectra rather than the chromatographic peaks.

(Figures S9 and S10) showed traces of non-PTFE compounds with –(CF2)n– series in their EI mass spectra as indicated with * in Figure 1C2. These peaks were considered to be nonpolymeric PFASs (Figure S7 and S9B), which was consistent with nonvolatile and volatile PFAS results (Table 1). Additional details with py-GC/MS chromatograms and mass spectra are included in the SI (Figures S3–S5).

The analysis of samples by py-GC/MS with the computation of similarities vs the py-GC/MS profiles of standards at the GC and MS levels using spectral contrast angles provided rapid identification of fluoropolymers and nonfluorinated polymers. The method currently implemented in Kendo[43,44] allows a specific moiety (e.g., CF_2) to be searched in order to extract simplified profiles out of complex raw data sets.[44] Multiple py-GC/MS profiles of standards were combined to compare the resulting profile with unknown samples for the simultaneous identification of different fluoropolymers.

Disposition of Fluorine. While others have speculated on the presence of fluoropolymer films or side-chain fluoropolymers,[21,38,55,56] the present study offers multiple lines of converging chemical evidence along with direct measurements by py-GC/MS that identifies and differentiates fluoropolymer films and side-chain fluoropolymers. Using a hierarchy of chemical characterization tools, the disposition of fluorine on firefighter turnout gear was categorized into three main groups: fluoropolymer (e.g., PTFE) films, side-chain fluoropolymers, and individual residual PFASs. The highest contribution of total fluorine and individual volatile PFAS concentrations is attributed to the PTFE film on the MBs, as identified by py-

https://doi.org/10.1021/acs.est.1c06322
Environ. Sci. Technol. 2022, 56, 974–983

GC/MS (Table 1). Pure PTFE should give a theoretical total fluorine concentration of 760,000 mg F/kg (eq S1). However, the total F concentrations on the MBs (43,700−122,000 mg F/kg) are all significantly lower than the theoretical value. If one assumes that the meta-aramid sublayer of the MB has a total fluorine concentration (5000 mg F/kg) similar to the OU layers (see FF1 and 4; Table 1), only ~15% of the total weight of the MB is PTFE (eq S2). Selection of 5000 mg F/kg is consistent with Schellenberger et al. who used a padding process to apply side-chain fluoropolymers to aramid-based fibers and achieved a mean total fluorine concentration of 4500 mg F/kg.[34] Thus, the fluorine of the PTFE film is diluted by the meta-aramid sublayers. The observed total fluorine on the treated para- and meta-aramid sublayers (Table 1) is consistent with the expected weight % F (0.04−0.25 wt % F) coverage imparted by the padding process.[57]

Side-chain fluoropolymers were likely added to the meta- and para-aramid sublayers in the MB, OU, and one TL sample (FF2). Because meta- and para-aramid are not inherently fluorinated, it is likely that the water-based "padding process" described in Holmquist et al.[21] was used to impart a fluorinated coating. Schellenberger et al.[34] also used the padding process to apply side-chain fluoropolymers onto fibers with an estimated thickness of 0.3 μm. Fluorinated side chains are bonded via an ester linkage to a nonfluorinated polymeric backbone[58] and are typically based on FTOHs or polyfluoroalkyl sulfonamidoethanols.[21] Quantification of n:2 FTOHs and *N*-methyl- and -ethyl-polyfluoroalkyl sulfonamidoethanols (Tables S12 and S13), which are used to make side-chain fluoropolymer monomers, which include the fluorotelomer acrylate and methacrylates (Table S13), are consistent with the chemistry associated with the padding process[21,59] and the synthesis of fluorotelomer-based side-chain fluoropolymers.[59] Sulfonamido-based acrylates and methacrylates were not measured in the present study but could be investigated in future studies as confirmation. The volatile PFASs detected in firefighter turnout gear may be due to incomplete synthesis or lack of purification.[30,59]

Individual PFASs (both nonvolatile and volatile) comprise a minor fraction of total fluorine, with some exceptions (the untreated TLs of FF1, 3, and 4). There are no apparent correlations between nonvolatile and total F, volatile and nonvolatile, or volatile and total F. However, there is a distinctly higher concentration of volatile PFASs associated with the MBs that contain PTFE. Thus, individual PFASs are not active ingredients in these textile treatment processes but are likely byproducts of incomplete reactions when synthesizing side-chain fluoropolymer monomers. Historically, side-chain fluoropolymer dispersions were allowed to be sold with up to 2% by weight of monomers per dry mass of polymer.[60] When side-chain fluoropolymer suspensions are applied and dried to textiles, loss of the residual PFASs and incomplete polymerizations typically result in residual monomers, smaller "polymers," and oliogmers.[30] Alternatively, cross-contamination during textile finishing processes could be the source of individual PFASs in textiles.[21] Because these are new turnout gear garments, the individual PFASs cannot be attributed to degradation or environmental degradation reactions. Although PFOA have been substituted in polymer production for the ammonium salt of hexafluoropropylene oxide dimer acid (HFPO-DA),[30] the substituted reagent is not detected in firefighter turnout pants herein (Table S11). Perfluoropolyether carboxylic acids (PFECAs) are another known substitute for PFNA in polymer production[30] but were not included in this study. Moreover, ammonium 4,8-dioxa-3*H*-perfluorononanoate (ADONA) is used as a PFECA processing aid and was not detected in firefighter turnout gear either (Table S11). Although nontarget PFAS analysis was not performed, such analysis could reveal additional compounds of concern, such as flame retardants and plasticizers[61,62] or newer polymerization aids. For example, Luo et al.[63] identified nonylphenol ethoxylates and octylphenol ethoxylates in cotton and polyester textiles.

If the layers of FF turnout gear are treated with side-chain fluorinated polymers based on ester linkages to a nonfluorinated polymeric backbone, then treatment with base-assisted extraction could result in elevated concentrations of individual PFASs reported in Peaslee et al.[17] For this reason, the higher individual PFAS concentrations reported by Peaslee et al. may represent the long-term oxidation of the nonvolatile PFAS concentrations rather than immediately accessible concentrations on new turnout gear. Furthermore, within the European union, regulations of PFOS in textiles should not exceed concentrations above 1 $\mu g/m^2$ of the coated material.[57] The only sample which had measured concentrations of PFOS above 1 $\mu g/m^2$ is the MB of FF1 and 4, while the remaining samples range from 0.18 to 1 $\mu g/m^2$.

Implications. A formal exposure assessment was beyond the scope of this study because we currently lack relevant parameters (e.g., partition coefficients) that could be used to characterize thermodynamic driving force, which is necessary to predict the rate of migration and therefore the dose associated with wearing firefighter turnout gear. For this reason, it is not yet possible to determine if the turnout gear is a significant source of occupational exposure to PFASs for firefighters. However, migration of impregnated chemicals from fabrics to skin is well established,[64−66] but not for PFASs, so further investigation of exposure is needed.

Dermal absorption of PFASs should be studied for not only PFCAs[67] but also other PFASs and especially volatile PFASs, particularly because concentrations of volatile PFASs were significantly higher than nonvolatile PFASs on the firefighter turnout gear. However, data gaps on dermal loading and absorptive flux must be filled before dermal exposure to PFASs from turnout gear can be reliably estimated. For a limited set of relatively lipid-soluble, semivolatile organic compounds, vapor uptake through skin may be comparable to, or exceed, inhalation exposure.[68,69] However, the relative importance of vapor uptake and inhalation has not been determined for semivolatile PFASs. Clothing can be an important mediating factor in dermal exposure. Clean clothing, even if gas permeable, can be at least initially protective through sorption of organic vapors, but may promote dermal absorption once that clothing becomes contaminated,[70,71] due to the enhanced mass transfer of the contaminant mass held close to the skin, suppression of volatilization, and warming of the skin. Fabric layers of turnout gear that are treated with side-chain fluoropolymers and individual PFASs may present the opportunity for elevated dermal exposure. Incidental ingestion of dust is another exposure route that should be considered for firefighters from turnout gear and dust in firehouses.[72]

Release of PFASs in durable water-repellant clothing due to heat, UV, and moisture needs to be assessed. van der Veen et al.[35] measured textile degradation under UV light in textiles, but the effect of heat and moisture is currently unknown. The impact of burning/high temperatures on firefighter turnout

https://doi.org/10.1021/acs.est.1c06322
Environ. Sci. Technol. 2022, 56, 974−989

gear has previously been performed,[73] but not yet in the context of PFASs. The effect of laundering on side-chain fluoropolymers and individual PFASs found in firefighter turnout gear should be analyzed as well. Mayer et al. in 2019 showed the impacts of laundering on removal of external contaminants such as flame retardants and PAHs from firefighter turnout gear.[74] Side-chain fluoropolymers associated with individual fibers are released during washing, as demonstrated in the case of outdoor jackets.[34] However, no information is available on the fate of PFASs, side-chain fluoropolymers, and PTFE associated with firefighter turnout gear as a result of laundering; therefore, further research is warranted. Firefighter turnout gear is recommended to be replaced after being worn for a period of 10 years.[75] Thus, firefighter turnout gear has potential to release and to act as a long-term source of individual PFASs to the environment upon disposal to landfills.[34] Degradation of fluoropolymer films and side-chain fluoropolymers under landfill conditions has not been investigated either and is another research gap to be fulfilled.

■ ASSOCIATED CONTENT

Supporting Information

The Supporting Information is available free of charge at https://pubs.acs.org/doi/10.1021/acs.est.1c06322.

Analytical method description; results of analytical performance for LC, GC, PIGE, and INAA; list of target nonvolatile and volatile PFAS analytes; list of suspect volatile PFAS analytes; whole method precision; nonvolatile PFAS surrogate standard recovery on blank, matrix blank, samples, and matrix spike; sublayers from FF layers and the amount analyzed by py-GC/MS; target PFCA, suflonate (PFS), miscellaneous electrofluorination (ECF) PFAS, and miscellaneous telomer PFAS concentrations; target and suspect FTOHs, Me- and Et-FOSA, MeFASE, EtFASEs, FTAcs, and FTMAcs concentrations; total fluorine concentrations by PIGE and INAA; workflow schematic for comparison by spectral contrast angles of pyGC/MS analysis; frequency of detection for nonvolatile and volatile PFASs in all firefighter turnout gear pants; similarity between the py-GC/MS profiles of a sample and a standard by spectral contrast angle; $-(CF_2)n-$ extracted profile; mass spectrum; remainders of $-(CF_2)n-$ extracted profiles; theoretical PTFE film concentration calculation; fraction of the PTFE film on the MB layer; total weight percent of F on non-PTFE layers; and conversion from $\mu g/m^2$ to ng/g (PDF)

■ AUTHOR INFORMATION

Corresponding Author

Jennifer A. Field − *Department of Environmental and Molecular Toxicology, Oregon State University, Corvallis, Oregon 97331, United States;* orcid.org/0000-0002-9346-4693; Email: jennifer.field@oregonstate.edu

Authors

Derek J. Muensterman − *Department of Chemistry, Oregon State University, Corvallis, Oregon 97331, United States;* orcid.org/0000-0002-7911-3563

Ivan A. Titaley − *Department of Environmental and Molecular Toxicology, Oregon State University, Corvallis, Oregon 97331, United States;* orcid.org/0000-0003-4683-1160

Graham F. Peaslee − *Department of Physics, University of Notre Dame, Notre Dame, Indiana 46556, United States;* orcid.org/0000-0001-6311-648X

Leah D. Minc − *Radiation Center, Oregon State University, Corvallis, Oregon 97311, United States*

Liliana Cahuas − *Department of Chemistry, Oregon State University, Corvallis, Oregon 97331, United States;* orcid.org/0000-0002-5973-2674

Alix E. Rodowa − *Hollings Marine Laboratory, National Institute of Standards and Technology, Charleston, South Carolina 29412, United States;* orcid.org/0000-0002-2650-0981

Yuki Horiuchi − *Research Institute for Sustainable Chemistry, National Institute of Advanced Industrial Science and Technology (AIST), Tsukuba, Ibaraki 305-8565, Japan*

Shogo Yamane − *Research Institute for Sustainable Chemistry, National Institute of Advanced Industrial Science and Technology (AIST), Tsukuba, Ibaraki 305-8565, Japan;* orcid.org/0000-0002-4025-8829

Thierry N.J. Fouquet − *Research Institute for Sustainable Chemistry, National Institute of Advanced Industrial Science and Technology (AIST), Tsukuba, Ibaraki 305-8565, Japan;* orcid.org/0000-0002-9473-9425

John C. Kissel − *Department of Environmental and Occupational Health Sciences, University of Washington, Seattle, Washington 98105, United States*

Courtney C. Carignan − *Department of Food Science and Human Nutrition, Department of Pharmacology and Toxicology, Michigan State University, East Lansing, Michigan 48824, United States*

Complete contact information is available at: https://pubs.acs.org/10.1021/acs.est.1c06322

Notes

The authors declare no competing financial interest.

■ ACKNOWLEDGMENTS

We thank the International Association of Fire Fighters for the donation of turnout gear. These opinions, recommendations, findings, and conclusions do not necessarily reflect the views or policies of NIST or the United States Government.

■ REFERENCES

(1) Keir, J. L. A.; Akhtar, U. S.; Matschke, D. M. J.; White, P. A.; Kirkham, T. L.; Chan, H. M.; Blais, J. M. Polycyclic aromatic hydrocarbon (PAH) and metal contamination of air and surfaces exposed to combustion emissions during emergency fire suppression: Implications for firefighters' exposures. *Sci. Total Environ.* **2020**, *698*, No. 134211.

(2) Driscoll, T. R.; Carey, R. N.; Peters, S.; Glass, D. C.; Benke, G.; Reid, A.; Fritschi, L. The Australian Work Exposures Study: Prevalence of Occupational Exposure to Formaldehyde. *Ann. Occup. Hyg.* **2016**, *60*, 132−138.

(3) Laitinen, J.; Makela, M.; Mikkola, J.; Huttu, I. Firefighters' multiple exposure assessments in practice. *Toxicol. Lett.* **2012**, *213*, 129−133.

(4) Laitinen, J. A.; Koponen, J.; Koikkalainen, J.; Kiviranta, H. Firefighters' exposure to perfluoroalkyl acids and 2-butoxyethanol present in firefighting foams. *Toxicol. Lett.* **2014**, *231*, 227−232.

(5) Rotander, A.; Toms, L. M. L.; Aylward, L.; Kay, M.; Mueller, J. F. Elevated levels of PFOS and PFHxS in firefighters exposed to aqueous film forming foam (AFFF). *Environ. Int.* **2015**, *82*, 28−34.

(6) Jin, C.; Sun, Y.; Islam, A.; Qian, Y.; Ducatman, A. Perfluoroalkyl Acids Including Perfluorooctane Sulfonate and Perfluorohexane Sulfonate in Firefighters. *J. Occup. Environ. Med.* **2011**, *53*, 324−328.
(7) McGuire, M. E.; Schaefer, C.; Richards, T.; Backe, W. J.; Field, J. A.; Houtz, E.; Sedlak, D. L.; Guelfo, J. L.; Wunsch, A.; Higgins, C. P. Evidence of remediation-induced alteration of subsurface poly- and perfluoroalkyl substance distribution at a former firefighter training area. *Environ. Sci. Technol.* **2014**, *48*, 6644−6652.
(8) Gill, R.; Hurley, S.; Brown, R.; Tarrant, D.; Dhaliwal, J.; Sarala, R.; Park, J. S.; Patton, S.; Petreas, M. Polybrominated Diphenyl Ether and Organophosphate Flame Retardants in Canadian Fire Station Dust. *Chemosphere* **2020**, *253*, 9.
(9) Shen, B.; Whitehead, T. P.; Gill, R.; Dhaliwal, J.; Brown, F. R.; Petreas, M.; Patton, S.; Hammond, S. K. Organophosphate flame retardants in dust collected from United States fire stations. *Environ. Int.* **2018**, *112*, 41−48.
(10) Shaw, S. D.; Berger, M. L.; Harris, J. H.; Yun, S. H.; Wu, Q.; Liao, C. Y.; Blum, A.; Stefani, A.; Kannan, K. Persistent organic pollutants including polychlorinated and polybrominated dibenzo-p-dioxins and dibenzofurans in firefighters from Northern California. *Chemosphere* **2014**, *102*, 87−87.
(11) Dobraca, D.; Israel, L.; McNeel, S.; Voss, R.; Wang, M. M.; Gajek, R.; Park, J. S.; Harwani, S.; Barley, F.; She, J. W.; Das, R. Biomonitoring in California Firefighters Metals and Perfluorinated Chemicals. *J. Occup. Environ. Med.* **2015**, *57*, 88−97.
(12) Trowbridge, J.; Gerona, R. R.; Lin, T.; Rudel, R. A.; Bessonneau, V.; Buren, H.; Morello-Frosch, R. Exposure to Perfluoroalkyl Substances in a Cohort of Women Firefighters and Office Workers in San Francisco. *Environ. Sci. Technol.* **2020**, *54*, 3363−3374.
(13) Grashow, R.; Bessonneau, V.; Gerona, R.; Wang, A.; Trowbridge, J.; Lin, T.; Buren, H.; Rudel, R. A.; Morello-Frosch, R. Integrating Exposure Knowledge and Serum Suspect Screening as a New Approach to Biomonitoring: An Application in Firefighters and Office Workers. *Environ. Sci. Technol.* **2020**, *54*, 4344−4355.
(14) Chen, J. J.; Tang, L. B.; Chen, W. Q.; Peaslee, G. F.; Jiang, D. Q. Flows, Stock, and Emissions of Poly- and Perfluoroalkyl Substances in California Carpet in 2000-2030 under Different Scenarios. *Environ. Sci. Technol.* **2020**, *54*, 6908−6918.
(15) Rewerts, J. N.; Morre, J. T.; Simonich, S. L. M.; Field, J. A. In-Vial Extraction Large Volume Gas Chromatography Mass Spectrometry for Analysis of Volatile PFASs on Papers and Textiles. *Environ. Sci. Technol.* **2018**, *52*, 10609−10616.
(16) Shinde, A.; Ormond, R. B. Headspace sampling-gas chromatograph-mass spectrometer as a screening method to thermally extract fireground contaminants from retired firefighting turnout jackets. *Fire Mater.* **2021**, *45*, 415−428.
(17) Peaslee, G. F.; Wilkinson, J. T.; McGuinness, S. R.; Tighe, M.; Caterisano, N.; Lee, S.; Gonzales, A.; Roddy, M.; Mills, S.; Mitchell, K. Another Pathway for Firefighter Exposure to Per- and Polyfluoroalkyl Substances: Firefighter Textiles. *Environ. Sci. Technol. Lett.* **2020**, *7*, 594−599.
(18) Itawi, R. K.; Aljobori, S. M.; Jalil, M.; Farhan, S. S.; Mheemeed, A.; Saaeed, K.; Ahmed, E. Determination of major, minor and trace-elements in textile dyes by INAA. *J. Radioan. Nucl. Ch. Ar.* **1991**, *149*, 339−343.
(19) Abel-Ghany, H. A. Study of radon, thoron and toxic elements in some textile dyes. *J. Radioanal. Nucl. Chem.* **2013**, *295*, 1365−1370.
(20) Schultes, L.; Peaslee, G. F.; Brockman, J. D.; Majumdar, A.; McGuinness, S. R.; Wilkinson, J. T.; Sandblom, O.; Ngwenyama, R. A.; Benskin, J. P. Total Fluorine Measurements in Food Packaging: How Do Current Methods Perform? *Environ. Sci. Technol. Lett.* **2019**, *6*, 73−78.
(21) Holmquist, H.; Schellenberger, S.; van der Veen, I.; Peters, G. M.; Leonards, P. E. G.; Cousins, I. T. Properties, performance and associated hazards of state-of-the-art durable water repellent (DWR) chemistry for textile finishing. *Environ. Int.* **2016**, *91*, 251−264.
(22) Shin, T.; Hajime, O.; Chuichi, W. *Pyrolysis-GC/MS Data Book of Synthetic Polymers - Pyrograms, Thermograms and MS of Pyrolyzates*; Elsevier: Amsterdam, 2012.
(23) Rial-Otero, R.; Galesio, M.; Capelo, J. L.; Simal-Gandara, J. A Review of Synthetic Polymer Characterization by Pyrolysis-GC-MS. *Chromatographia* **2009**, *70*, 339−348.
(24) Sabatini, F.; Nacci, T.; Degano, I.; Colombini, M. P. Investigating the composition and degradation of wool through EGA/MS and Py-GC/MS. *J. Anal. Appl. Pyrolysis* **2018**, *135*, 111−121.
(25) Cho, M. S.; Kim, M. D.; Park, S.; Yoon, K. J.; Nam, J. D.; Lee, J. H.; Lee, Y. Analysis of cotton/polyester fabrics using pyrolysis gas chromatograpy. *Polymer* **2003**, *27*, 271−274.
(26) Kissa, E., *Fluorinated, surfactants: Synthesis, Properties, and Applications*; Marcel Dekker: New York, 1994; Vol. *50*.
(27) Dolan, M. J.; Blackledge, R. D.; Jorabchi, K. Classifying single fibers based on fluorinated surface treatments. *Anal. Bioanal. Chem.* **2019**, *411*, 4775−4784.
(28) Matsui, K.; Ishimura, T.; Mattonai, M.; Iwai, I.; Watanabe, A.; Teramae, N.; Ohtani, H.; Watanabe, C. Identification algorithm for polymer mixtures based on Py-GC/MS and its application for microplastic analysis in environmental samples. *J. Anal. Appl. Pyrolysis* **2020**, *149*, 9.
(29) Henry, B. J.; Carlin, J. P.; Hammerschmidt, J. A.; Buck, R. C.; Buxton, L. W.; Fiedler, H.; Seed, J.; Hernandez, O. A critical review of the application of polymer of low concern and regulatory criteria to fluoropolymers. *Integr. Environ. Assess. Manag.* **2018**, *14*, 316−334.
(30) Lohmann, R.; Jaward, F.; Durham, L.; Barber, J.; Ockenden, W.; Jones, K.; Bruhn, R.; Lakaschus, S.; DAchs, J.; Booij, A. Potential contamination of shipboard air samples by diffusive emissions of PCBs and other organic pollutants: implications and solutions. *Environ. Sci. Technol.* **2004**, *38*, 3965−3970.
(31) Washington, J. W.; Jenkins, T. M.; Rankin, K.; Naile, J. E. Decades-Scale Degradation of Commercial, Side-Chain, Fluorotelomer-Based Polymers in Soils and Water. *Environ. Sci. Technol.* **2015**, *49*, 915−923.
(32) Washington, J. W.; Jenkins, T. M. Abiotic Hydrolysis of Fluorotelomer-Based Polymers as a Source of Perfluorocarboxylates at the Global Scale. *Environ. Sci. Technol.* **2015**, *49*, 14129−14135.
(33) Washington, J. W.; Naile, J. E.; Jenkins, T. M.; Lynch, D. G. Characterizing Fluorotelomer and Polyfluoroalkyl Substances in New and Aged Fluorotelomer-Based Polymers for Degradation Studies with GC/MS and LC/MS/MS. *Environ. Sci. Technol.* **2014**, *48*, 5762−5769.
(34) Schellenberger, S.; Jonsson, C.; Mellin, P.; Levenstam, O. A.; Liagkouridis, I.; Ribbenstedt, A.; Hanning, A. C.; Schultes, L.; Plassmann, M. M.; Persson, C.; Cousins, I. T.; Benskin, J. P. Release of Side-Chain Fluorinated Polymer-Containing Microplastic Fibers from Functional Textiles During Washing and First Estimates of Perfluoroalkyl Acid Emissions. *Environ. Sci. Technol.* **2019**, *53*, 14329−14338.
(35) van der Veen, I.; Hanning, A. C.; Stare, A.; Leonards, P. E. G.; de Boer, J.; Weiss, J. M. The effect of weathering on per- and polyfluoroalkyl substances (PFASs) from durable water repellent (DWR) clothing. *Chemosphere* **2020**, *249*, No. 126100.
(36) Interstate Technology & Resource Council Use and Measurement of Mass Flux and Mass Discharge; August, 2010; p 89.
(37) Wan, K. X.; Vidavsky, I.; Gross, M. L. Comparing similar spectra: From similarity index to spectral contrast angle. *J. Am. Soc. Mass Spectrom.* **2002**, *13*, 85−88.
(38) Robel, A. E.; Marshall, K.; Dickinson, M.; Lunderberg, D.; Butt, C.; Peaslee, G.; Stapleton, H. M.; Field, J. A. Closing the Mass Balance on Fluorine on Papers and Textiles. *Environ. Sci. Technol.* **2017**, *51*, 9022−9032.
(39) Schwichtenberg, T.; Bogdan, D.; Carignan, C. C.; Reardon, P.; Rewerts, J.; Wanzek, T.; Field, J. A. PFAS and Dissolved Organic Carbon Enrichment in Surface Water Foams on a Northern US Freshwater Lake. *Environ. Sci. Technol.* **2020**, *54*, 14455−14464.

https://doi.org/10.1021/acs.est.1c06322
Environ. Sci. Technol. 2022, 56, 982−

Supporting Information

Disposition of Fluorine on New Firefighter Turnout Gear

Derek J. Muensterman[a], Ivan A. Titaley[b], Graham F. Peaslee[c], Leah D. Minc[d], Liliana Cahuas[a], Alix E. Rodowa[e], Yuki Horiuchi[f], Shogo Yamane[f], Thierry N.J. Fouquet[f], John C. Kissel[g], Courtney C. Carignan[h], Jennifer A. Field[b]

[a]Department of Chemistry, Oregon State University, Corvallis, Oregon 97331, United States
[b]Department of Environmental and Molecular Toxicology, Oregon State University, Corvallis, Oregon 97331, United States
[c]Department of Physics, University of Notre Dame, Notre Dame, Indiana 46556, United States
[d]Radiation Center, Oregon State University, Corvallis, Oregon 97311, United States
[e]Hollings Marine Laboratory, National Institute of Standards and Technology, Charleston, South Carolina 29412, United States
[f]Research Institute for Sustainable Chemistry, National Institute of Advanced Industrial Science and Technology (AIST), 1-1-1 Higashi, Tsukuba, Ibaraki 305-8565, Japan
[g]Department of Environmental and Occupational Health Sciences, University of Washington, Seattle, Washington 98105, United States
[h]Department of Food Science and Human Nutrition, Department of Pharmacology and Toxicology, Michigan State University, East Lansing, Michigan 48824, United States

Table of Contents **Page**

Experimental Methods

Standards and Reagents. For LC-MS/MS analysis, HPLC grade water (>99%, high purity, Burdick and Jackson brand) was purchased from Fisher Scientific (Hampton, NH). Ammonium acetate (regent grade, Macrom Chemicals) was purchased from VWR (Radnor, PA). MO). Methanol (>99%, LC/MS grade) was purchased from Fisher Scientific (Hampton, NH). Ethylene Glycol (ReagentPlus® ≥99%) was purchased from Sigma-Aldrich (St. Louis, MO) For GC-MS analysis, methanol (≥99.5%, pesticide residue analysis grade) was purchased from VWR (Radnor, PA).

Non-volatile PFAS Analysis by Liquid Chromatography Quadrupole Time of Flight. Extraction of PFAS from firefighter turnout gear followed a similar procedure as used in Robel et al.[1] Sample preparation consisted of using methanol-rinsed scissors to cut 2 × 2 cm^2 pieces of material in order to allowed free movement of the material within the centrifuge tube. 0.9 ng of each mass-labeled surrogate were spiked into all 15 mL polypropylene tubes (Fisher Brand, Disposable Centrifuge Tube, 15 mL plug seal cap, Cat. No. 05-539-4) prior to extraction. Methanol (MeOH) was heated to 60-65°C in a water bath prior to extraction. A glass Pasteur pipette (Fisherbrand 5 ¾ " Disposable Pasteur Pipets, Cat. No. 13-678-20A) was used to aliquot 3.3 mL of MeOH into a 10 mL graduated cylinder and transferred to a material sample tube. The 15 mL centrifuge tubes were immediately capped to prevent loss of solvent. Following the 3.3 mL aliquots of MeOH, each tube was placed on a wrist action shaker at a 10° rotation for ten min (Burrell, Model 75, Pittsburgh, PA). Samples were then centrifuged (Thermo Scientific, model Sorvall Legend X1, Waltham, Massachusetts) at 2808g for ten min at ambient temperature. Supernatant was transferred to the second centrifuge tube. The extraction was repeated twice more for a target total volume of 10 mL. Extracts were frozen overnight in a -20°C freezer in order to precipitate any other particulate matter remaining in the extract. Extracts were taken out of the freezer and centrifuged at 2808g for ten min, after which 30 µL of ethylene glycol was added to each centrifuge tube and concentrated under nitrogen to a final volume of 150 µL. Analysis consisted of a 50 µL aliquot of each extract into 300 µL conical vials (VWR, PP Vial Clear, 9-425 screw thread 300 µL) with 0.30 ng of each mass-labelled internal standard. Extracts were stored at -20°C until analysis.

Chromatographic separations were achieved using an Agilent 1260 HPLC (Santa Clara, CA). Aliquots of 100 μL were injected onto a Zorbax Eclipse XDB-C8 (4.6 x 20 mm, 3.5 µm) guard column fitted with a Zorbax Eclipse Plus analytical column (4.6 x 75 mm, 3.5µm; Agilent) as modified after Backe et al.[2] The aqueous mobile phase (A) was 10 mM ammonium acetate (Fisher Scientific) in 3% v/v HPLC-grade methanol in HPLC-grade water and the organic mobile phase (B) was HPLC-grade MeOH.

A SCIEX X500R QToF-MS/MS system (Framingham, MA) was operated in negative mode and in electrospray ionization (ESI-) mode. Data were collected under SWATH® data-independent acquisition for both TOF-MS and MS/MS modes. PFBA and MPFBA were analyzed in MS/MS mode to reduce background. Over the entirety of the data acquisition period, precursor ion data (TOF-MS) were collected over an m/z range of 100 Daltons (Da; TOF start mass) to 1250 Da (TOF stop). The accumulation time was 200 ms and the ion spray voltage was -4500 V. The source and gas parameters included: a source temperature of 550 °C, ion source gasses at 60 psi, curtain gas at 35 psi, and collision gas at 10 psi. The declustering potential was -20 V (with 0 V spread) and the collision energy was -5 V (with 0 V spread). Product ion scan (TOF-MS/MS) data were collected for a m/z range from 50 Da (TOF start mass) to 1200 Da. The accumulation time for each SWATH® window was 50 ms.

Method accuracy and precision were determined by spiking four replicate blank polyethylene (PE) films with 2.25 ng of all target analytes (Table S1) and extracted as outlined above. Polyethylene (PE) film was used as representative sample due to the difficulty in finding non-fluorinated durable water repellant fabric. To provide a measure of precision on an actual firefighter layer, FF1-OU was extracted and analyzed in quadruplicate. The method limits of detection (LOD) was determined according to Vial and Jardy.[3] Ten 2 × 2 cm^2 PE films were spiked with all non-

volatile target analytes ranging between 0.0045 to 0.45 ng and extracted and analyzed as described above. The method LOD was calculated based on linear regression with $1/x$ weighting and method limits of quantification (LOQ) was calculated by multiplying method LOD with 3.3.

Volatile PFAS Analysis by Gas Chromatography-Mass Spectrometry. Extraction of volatile PFAS from firefighter turnout gear followed the same procedure as used in Rewerts et al.[4] with a few modifications. Sample preparation consisted of using MeOH-rinsed scissors to cut 1.5 × 1.5 cm^2 pieces of material. Samples were weighed and placed in 1.5 mL autosampler vials, MeOH was added, internal standards were spiked, and vials were sonicated for 30 min at 25°C. The samples were directly analysed without any further clean-up.

Sample extracts were analysed using GC-concurrent solvent recondensation large volume spitless injection coupled with mass spectrometry using 10 µL of the extracts injected in splitless mode with inlet temperature of 280°C. A 4 mm i.d. single taper Topaz inlet liner with 15 mg deactivated quartz wool (Restek, Bellefonte, PA) was used. Helium was used as the carrier gas in a constant flow mode of 1.0 mL/min. Separations were performed using an Agilent deactivated, fused silica tubing capillary column (5 m × 0.53 mm i.d.) connected to a Restek Rxi-624Sil MS capillary column (30 m ×0.25 mm i.d., 1.40 µm film thickness). The GC oven temperature program was as follows: 50°C for 2.0 min, ramped to 188°C at a rate of 5.0°C/min, then ramped to 250°C at a rate of 15°C/min. The Agilent 6890 GC was connected to an Agilent 5973N MS that was operated in positive chemical ionization mode in selected ion monitoring mode with methane as the reagent gas at a flow rate of 1 mL/min.

Method accuracy and precision for volatile PFAS were determined by spiking three PE film replicates to give a final concentration of 50 pg/µL of FTOHs, FOSAs, and FOSEs target analytes and 5.0 pg/µL of FTAcs and FTMAcs target analytes. Triplicate samples of FF1-OU were extracted to obtain a measure precision for an actual firefighter layer. The method LOD for volatile PFAS was determined according to Vial and Jardy. ^{3}Ten 1.5 × 1.5 cm^2 PE films were spiked with target volatile PFAS ranging between 0.037 to 150 ng of FTOHs, FOSAs, FOSEs and 0.00075 to 15 ng of FTACs and FTMAcs, and were extracted and analyzed as described above. Method LOD and LOQ were calculated as described above.

Total Fluorine by Particle-Induced Gamma Ray Emission. In Rodowa et al., an inorganic fluorine calibration curve was used to determine the total fluorine in materials.[5] However, in this study, was determined based on an organic fluorine calibration curve. The total fluorine in nmol F/cm^2 obtained from the conversion with organic fluorine calibration curve were compared with total fluorine in nmol F/cm^2 obtained based on the inorganic fluorine calibration curve and density of the materials. The ratio of the total fluorine between the organic and inorganic calibration curves ranged from 0.1 to 22×.

Total Fluorine Analysis by Instrumental Neutron Activation Analysis. Decay time varied according to the initial level of F activity in the sample, and ranged from ca. 25-60 s. Detector dead times were often quite high due to the presence of other short half-life isotopes, potentially leading to peak broadening; accordingly, peak area calculations were verified through interactive peak-fitting. Element concentrations were determined through direct comparison with the standards based on decay-corrected activities of the 1633.6 keV peak. Possible interferences to this peak from the fast neutron reaction $^{23}Na(n,\alpha)^{20}F$ were evaluated using the average of two replicates of a single-element Na standard. The measured ratio of interference at 1633.6 keV to the characteristic 1368.6 keV γ-ray peak for Na was used to correct interference in the samples; interference corrections ranged from <1% to 6%.

Bulk Characterization by Pyrolysis-GC/MS. The pyrolyser temperature was set at 600°C. The oven temperature initially set at 40°C was linearly increased at 20°C/min up to 320 °C and maintained for 14 min (total experiment time: 30 min). Mass spectra were recorded using a JMS-T200GC mass spectrometer (JEOL, Japan) equipped with an electron ionization (EI) source and a high-resolution time-of-flight mass analyzer with ~1.9 scans per second (TOF, resolving power ~10

000 for m/z < 1000). The instrument is routinely calibrated using the EI mass spectrum of perfluorotributylamine (19 peaks between m/z 69 and m/z 614) and fine-tuned using a peak from 1,3-dibromotetrafluorobenzene standard at m/z 305.8297 before analyzing the samples. Errors of mass measurements that may gradually occur during py-GC/MS measurements are corrected using the peak from hexamethylcyclotrisiloxane at m/z 207.0324 continually detected as a background signal due to column bleed.

Procedure for extraction of –(CF$_2$)n- series and similarity. The -$(CF_2)_n$- extracted profile for the black coating from FF1 MB displays an intense and broad peak at the early elution times while very minor peaks are barely visible in the –(CF_2)- extracted profile for the white fabric. Artifact peaks are due to background signals of very low abundance in the mass spectra which are spaced by only one ~49.9968 Da from more intense signals but which cannot be considered as true $(CF_2)_n$ series due to the absence of congener.

Similarity between the py-GC/MS profiles of a sample and a standard. Chosen criteria: spectral-contrast angle "Θ" (angle between two mass spectra considered as vectors)[6]; $\Theta = 0^0$ → perfectly aligned vectors → identical mass spectra; $\Theta = 90^0$ → fully orthogonal vectors → completely different mass spectra.

Implementation in kendo for py-GC/MS profiles. Concatenation of scans from one profile using a user-defined width generating a summed mass spectrum to overcome the inevitable variations of retention time from one experiment to another for the same chemical (intrinsic variability of a device) in replacement of the retention time shifting[7]. Chosen width for all the profiles: 0.03 min corresponding to 3 scans, 1160 summed mass spectra for each py-GC/MS profile. Calculation of the 1160 spectral-contrast-angles "Θ" between the summed mass spectra from the py-GC/MS profile of the sample and the standard. Grouping of the summed mass spectra by their Θ angle if inferior to a chosen criterion to recover a list of highly similar py-GC peaks and mass spectra. Chosen criterion of high similarity: $\Theta \leq 5^0$. A summed mass spectrum from the combined scans with Θ angles $<5^0$deg is finally computed for the two py-GC/MS profiles of the sample and the standard. For sake of simplicity the mass spectra of the matching GC peaks are not presented – data available upon request.

Results and Discussion

Non-volatiles Extraction and Analysis by LC-qTOF. Method accuracy for non-volatile PFAS ranged between 41 and 310%, while method precision ranged between 1.2 and 61% (Table S4). FF1-OU precision ranged between 44-122%. Internal standard recovery ranged between 29-120% and 33-130% for MPFOA and MPFOS, respectively (Table S5). Method LOD ranged from 0.0099 to 0.18 μg/m^2 and method LOQ ranged from 0.033 – 0.58 μg/m^2 (Table S4).

Volatiles Extraction and Analysis by GC-MS. Method accuracy for volatile PFAS ranged between 28 and 120%, while method precision ranged between 0.36 and 4.4% (Table S4). FF1-OU precision ranged between 13 – 22%. Method LOD for volatile PFAS ranged between 0.21 and 8.2 μg/m^2 and method LOQ ranged between 0.7 and 27 μg/m^2 (Table S6).

Total Fluorine Analysis by PIGE. The accuracy of PIGE ranged between 96 and 106%, while the precision was determined to be ± 5.4%.[8] The method quantification limit for PIGE was 16.2 ppm F.[8]

Total Fluorine Analysis by INAA. INAA precision, determined based on the CaF_2 standards, was calculated to be 0.7%. Detection limits for fluorine by INAA are strongly dependent on sample matrix and are adversely affected by the presence of other short half-life isotopes, notably ^{28}Al, ^{38}Cl, and/or ^{80}Br. In the absence of high background counts, an F concentration of 13 ± 5 ppm was detected in a 1.4 g sample.

Table S1: List of target non-volatile PFAS analytes.[1]

Analyte	Acronym	Neutral Molecular Formula	Surrogate Standard
Perfluoro-n-butanoic acid	PFBA[2]	$C_4HO_2F_7$	MPFBA
Perfluoro-n-petnanoic acid	PFPeA	$C_5HO_2F_9$	M3PFPeA
Perfluoro-n-hexanoic acid	PFHxA	$C_6HO_2F_{11}$	M2PFHxA
Perfluoro-n-heptanoic acid	PFHpA	$C_7HO_2F_{13}$	M4PFHpA
Perfluoro-n-octanoic acid	PFOA	$C_8HO_2F_{15}$	M4PFOA
Perfluoro-n-nonanoic acid	PFNA	$C_9HO_2F_{17}$	M5PFNA
Perfluoro-n-decanoic acid	PFDA	$C_{10}HO_2F_{19}$	MPFDA
Perfluoro-n-undecanoic acid	PFUdA	$C_{11}HO_2F_{21}$	MPFUdA
Perfluoro-n-dodecanoic acid	PFDoA	$C_{12}HO_2F_{23}$	MPFDoA
Perfluoro-n-tridecanoic acid	PFTrDA	$C_{13}HO_2F_{25}$	MPFDoA
Perfluoro-n-tetradecanoic acid	PFTeDA	$C_{14}HO_2F_{27}$	M2PFTeDA
Perfluoro-n-hexadecanoic acid	PFHxDA	$C_{16}HO_2F_{31}$	M2PFHxDA
Perfluoropropane sulfonate	PFPrS	$C_3HO_3SF_7$	M3PFBS
Perfluorobutane sulfonate	PFBS	$C_4HO_3SF_9$	M3PFBS
Perfluoropentane sulfonate	PFPeS	$C_5HO_3SF_{11}$	M3PFBS
Perfluorohexane sulfonate	PFHxS	$C_6HO_3SF_{13}$	MPFHxS
Perfluoroheptane sulfonate	PFHpS	$C_7HO_3SF_{15}$	MPFHxS
Perfluorooctane sulfonate	PFOS	$C_8HO_3SF_{17}$	MPFOS
Perfluorononane sulfonate	PFNS	$C_9HO_3SF_{19}$	MPFOS
Perfluorodecane sulfonate	PFDS	$C_{10}HO_3SF_{21}$	MPFOS
Perfluorododecane sulfonate	PFDoS	$C_{12}HO_3SF_{25}$	MPFOS
8-chloro-perfluorooctane sulfonate	Cl-PFOS	$C_8HClF_{16}SO_3$	MPFOS
Perfluoroethylcyclohexane sulfonate	PFEtCHxS	$C_8HO_3SF_{15}$	MPFHxS
Perfluorobutane sulfonamide	FBSA	$C_4H_2O_2NSF_9$	M8FOSA
Perfluorohexane sulfonamide	FHxSA	$C_6H_2O_2NSF_{13}$	M8FOSA
Perfluorooctane sulfonamide	FOSA	$C_8H_2O_2NSF_{17}$	M8FOSA
N-methylperfluoro-1-octane sulfonamide	MeFOSA	$C_9H_4O_2NSF_{17}$	d-N-MeFOSA-M
N-ethylperfluoro-1-octane sulfonamide	EtFOSA	$C_{10}H_6O_2NSF_{17}$	d-N-EtFOSA-M
Perfluorooctane sulfonamido acetic acid	FOSAA	$C_{10}H_4O_4NSF_{17}$	d_3-N-MeFOSAA
N-methylperfluorooctane sulfonamido acetic acid	MeFOSAA	$C_{11}H_6O_4NSF_{17}$	d_3-N-MeFOSAA
N-ethylperfluorooctane sulfonamido acetic acid	EtFOSAA	$C_{12}H_8O_4NSF_{17}$	d5-N-EtFOSAA
4:2 fluorotelomer sulfonate	4:2 FTS	$C_6H_5O_3SF_9$	M2-4:2FTS
6:2 fluorotelomer sulfonate	6:2 FTS	$C_8H_5O_3SF_{13}$	M2-6:2FTS
8:2 fluorotelomer sulfonate	8:2 FTS	$C_{10}H_5O_3S_{F17}$	M2-8:2FTS
10:2 fluorotelomer sulfonate	10:2 FTS	$C_{12}H_5O_3SF_{21}$	M2-8:2FTS
6:2 fluorotelomer carboxylic acid	6:2 FTCA	$C_8H_3O_2F_{13}$	M6:2FTA
8:2 fluorotelomer carboxylic acid	8:2 FTCA	$C_{10}H_3O_2F_{17}$	M8:2FTA
10:2 fluorotelomer carboxylic acid	10:2 FTCA	$C_{12}H_3O_2F_{21}$	M10:2FTA
3:3 fluorotelomer carboxylic acid	3:3 FTCA	$C_6H_5O_2F_7$	M6:2FTA

5:3 fluorotelomer carboxylic acid	5:3 FTCA	$C_8H_5O_2F_{11}$	M8:2FTA
7:3 fluorotelomer carboxylic acid	7:3 FTCA	$C_{10}H_5O_2F_{15}$	M10:2FTA
2H-Perfluoro-2-octenoic acid (6:2)	6:2 UFTCA	$C_8H_2O_2F_{12}$	M6:2FTUA
2H-Perfluoro-2-decenoic acid (8:2)	8:2 UFTCA	$C_{10}H_2O_2F_{16}$	M8:2FTUA
Dodecafluoro-3H-4,8-dioxanoate	ADONA	$C_7H_2O_4F_{12}$	M5PFNA
9-chlorohexadecafluoro-3-oxanonane-1-sulfonate	9Cl-PF3ONS	$C_8HF_{16}ClSO_4$	MPFOS
11-chloroeicosafluoro-3-oxaundecane-1-sulfonate	11-PF3OUdS	$C_{10}HF_{20}ClSO_4$	MPFOS
hexafluoropropylene oxide-dimer acid	HFPO-DA	$C_6HF_{11}O_3$	MHFPO-DA
bis(1H,1H,2H,2H-perfluorooctyl)phosphate	6:2 diPAP	$C_{16}H_9F_{26}O_4P$	M4 8:2 diPAP
bis(1H,1H,2H,2H-perfluorodecyl)phosphate	8:2 diPAP	$C_{20}H_9F_{34}O_4P$	M4 8:2 diPAP
Bis-[2-(N-ethyleperflurooctane-1-sulfonamido)ethyl] phosphate	diSAmPAP	$C_{24}H_{19}F_{34}N_2O_8PS_2$	M4 8:2 diPAP

[1][M-H]$^-$ adducts were used for quantification

[2]MRM transitions of 213 → 169 and 217 → 172 were used for quantification of PFBA and MPFBA, respectively, to reduce background.

Table S2: List of target volatile PFAS analytes.

Analyte	Acronym	Neutral Molecular Formula	Surrogate Standard
4:2 fluorotelomer alcohol	4:2 FTOH	$C_6H_5OF_9$	MFBET
6:2 fluorotelomer alcohol	6:2 FTOH	$C_8H_5OF_{13}$	MFHET
8:2 fluorotelomer alcohol	8:2 FTOH	$C_{10}H_5OF_{17}$	M2FOET
10:2 fluorotelomer alcohol	10:2 FTOH	$C_{12}H_5OF_{21}$	MFDET
12:2 fluorotelomer alcohol	12:2 FTOH	$C_{14}H_5OF_{25}$	MFDET
N-methyl perfluoroalkane sulfonamide	MeFOSA	$C_9H_4NO_2SF_{17}$	d_3-N-MeFOSA-M
N-ethyl perfluoro-1-octane sulfonamide	EtFOSA	$C_{10}H_6NO_2SF_{17}$	d_5-N-EtFOSA-M
N-methyl perfluorooctane sulfonamidoethanol	MeFOSE	$C_{11}H_8NO_3SF_{17}$	d_7-N-MeFOSE-M
N-ethyl perfluorooctane sulfonamidoethanol	EtFOSE	$C_{12}H_{10}NO_3SF_{17}$	d_9-N-EtFOSE-M
4:2 fluorotelomer acrylate	4:2 FTAc	$C_9H_7F_9O_2$	d_3-6:2 FTAc
6:2 fluorotelomer acrylate	6:2 FTAc	$C_{11}H_7F_{13}O_2$	d_3-6:2 FTAc
8:2 fluorotelomer acrylate	8:2 FTAc	$C_{13}H_7F_{17}O_2$	d_3-6:2 FTAc
10:2 fluorotelomer acrylate	10:2 FTAc	$C_{15}H_7F_{21}O_2$	d_3-6:2 FTAc
6:2 Fluorotelomer methylacrylate	6:2 FTMAc	$C_{12}H_9F_{13}O_2$	d_5-6:2 FTMAc
8:2 Fluorotelomer methylacrylate	8:2 FTMAc	$C_{14}H_9F_{17}O_2$	d_5-6:2 FTMAc

Table S3: List of suspect volatile PFAS analytes.

Analyte	Acronym	Neutral Molecular Formula	Surrogate Standard
14:2 fluorotelomer alcohol	14:2 FTOH	$C_{16}H_5OF_{29}$	MFDET
N-methyl perfluoropropane sulfonamidoethanol	MeFPrSE	$C_6H_8NO_3SF_7$	d_7-N-MeFOSE-M
N-methyl perfluorobutane sulfonamidoethanol	MeFBSE	$C_7H_8NO_3SF_9$	d_7-N-MeFOSE-M
N-methyl perfluoropentane sulfonamidoethanol	MeFPeSE	$C_8H_8NO_3SF_{11}$	d_7-N-MeFOSE-M
N-methyl perfluorohexane sulfonamidoethanol	MeFHxSE	$C_9H_8NO_3SF_{13}$	d_7-N-MeFOSE-M
N-methyl perfluoroheptane sulfonamidoethanol	MeFHpSE	$C_{10}H_8NO_3SF_{15}$	d_7-N-MeFOSE-M
N-ethyl perfluoroethane sulfonamidoethanol	EtFEtSE	$C_6H_{10}NO_3SF_5$	d_9-N-EtFOSE-M
N-ethyl perfluoropropane sulfonamidoethanol	EtFPrSE	$C_7H_{10}NO_3SF_7$	d_9-N-EtFOSE-M
N-ethyl perfluorobutane sulfonamidoethanol	EtFBSE	$C_8H_{10}NO_3SF_9$	d_9-N-EtFOSE-M
N-ethyl perfluoropentane sulfonamidoethanol	EtFPeSE	$C_9H_{10}NO_3SF_{11}$	d_9-N-EtFOSE-M
N-ethyl perfluorohexane sulfonamidoethanol	EtFHxSE	$C_{10}H_{10}NO_3SF_{13}$	d_9-N-EtFOSE-M
N-ethyl perfluoroheptane sulfonamidoethanol	EtFHpSE	$C_{11}H_{10}NO_3SF_{15}$	d_9-N-EtFOSE-M
4:2 fluorotelomer iodide	4:2 FTI	$C_6H_4F_9I$	d_5-6:2 FTMAc
6:2 fluorotelomer iodide	6:2 FTI	$C_8H_4F_{13}I$	d_5-6:2 FTMAc
8:2 fluorotelomer iodide	8:2 FTI	$C_{10}H_4F_{17}I$	d_5-6:2 FTMAc
10:2 fluorotelomer iodide	10:2 FTI	$C_{12}H_4F_{21}I$	d_5-6:2 FTMAc
Perfluorobutyl iodide	PFBI	C_4F_9I	d_5-6:2 FTMAc
Perfluorohexyl iodide	PFHxI	$C_6F_{13}I$	d_5-6:2 FTMAc
Perfluorooctyl iodide	PFOI	$C_8F_{17}I$	d_5-6:2 FTMAc
Perfluorodecyl iodide	PFDI	$C_{10}F_{21}I$	d_5-6:2 FTMAc
6:2 fluorotelomer olefin	6:2 FTO	$C_8H_3F_{13}$	d_5-6:2 FTMAc
8:2 fluorotelomer olefin	8:2 FTO	$C_{10}H_3F_{17}$	d_5-6:2 FTMAc
10:2 fluorotelomer olefin	10:2 FTO	$C_{12}H_3F_{21}$	d_5-6:2 FTMAc
12:2 fluorotelomer olefin	12:2 FTO	$C_{14}H_3F_{25}$	d_5-6:2 FTMAc

Table S4: Whole method precision (% RSD), whole method accuracy (% average recovery), method LOD, and method LOQ based on polytheylene film (sample matrix) spiked with non-volatile PFAS. 5000 ng/L non-volatile PFAS were spiked for whole method precision and whole method accuracy ($n = 4$). 10 – 1000 ng/L non-volatile PFAS were spiked for method LOD ($n = 8$). Method LOQ was calculated by multiplying method LOD with 3.3.

Analyte	Whole method precision (% RSD)	Whole method accuracy (% average recovery)	Method LOD (µg/m²)	Method LOQ (µg/m²)
PFBA	6.3	100	0.021	0.07
PFPeA	6.2	86	0.055	0.18
PFHxA	6.1	110	0.044	0.15
PFHpA	6	95	0.037	0.12
PFOA	5	93	0.035	0.12
PFNA	5.5	92	0.043	0.14
PFDA	7.8	120	0.021	0.071
PFUdA	2.5	120	0.033	0.11
PFDoA	2.7	100	0.072	0.24
PFTrDA	22	86	0.031	0.1
PFTeDA	3.9	100	0.012	0.04
PFHxDA	1.2	100	0.043	0.14
PFPrS	6.7	85	0.03	0.1
PFBS	3.2	91	0.0099	0.033
PFPeS	5.5	81	0.026	0.087
PFHxS	3.2	83	0.021	0.071
PFHpS	6.1	81	0.033	0.11
PFOS	6	89	0.015	0.05
PFNS	7.2	98	0.027	0.089
PFDS	2.7	94	0.032	0.11
PFDoS	14	88	0.026	0.087
Cl-PFOS	7.2	98	0.022	0.073
PFEtCHxS	4.8	81	0.021	0.068
FBSA	4.5	95	0.053	0.18
FHxSA	9.7	88	0.039	0.13
FOSA	7.7	85	0.037	0.12
MeFOSA	11	100	0.058	0.19
EtFOSA	4.1	120	0.053	0.18
FOSAA	6.2	130	0.037	0.12
MeFOSAA	14	110	0.08	0.27
EtFOSAA	23	120	0.027	0.091
4:2 FTS	10	110	0.051	0.17
6:2 FTS	5.1	95	0.072	0.24
8:2 FTS	11	110	0.08	0.27
10:2 FTS	15	310	0.055	0.18
3:3 FTCA	30	96	0.16	0.52
5:3 FTCA	35	96	0.12	0.4
7:3 FTCA	32	120	0.18	0.58
6:2 FTCA	31	160	0.098	0.33

8:2 FTCA	23	82	0.14	0.47
10:2 FTCA	61	130	0.12	0.42
6:2 UFTCA	17	92	0.12	0.4
8:2 UFTCA	16	130	0.14	0.47
ADONA	8.4	80	0.04	0.13
9Cl-PF3ONS	9.8	96	0.02	0.068
11l-PF3OUdS	4.1	91	0.029	0.096
HFPO-DA	23	110	0.079	0.26
6:2diPAP	30	41	0.055	0.18
8:2diPAP	20	110	0.079	0.26
diSAmPAP	31	61	0.03	0.1

Table S5: Non-volatile PFAS surrogate standards recovery on blank, matrix blank, samples, and matrix spike. Polyethylene film was used for matrix blank ($n = 3$) and matrix spike ($n = 3$). Data for matrix blank, matrix spike, and FF1-OU ($n = 4$) were provided in average±standard deviation.

Sample Name	M4PFOA/M8PFOA (% recovery)	MPFOS/M8PFOS (% recovery)
Processing Blank	70	75
Matrix Blank	85±9.0	89±6.9
FF1-OU	80±19.8	81±19.6
FF1-MB	71	100
FF1-TL	60	61
FF2-OU	32	41
FF2-MB	38	57
FF2-TL	71	73
FF3-OU	80	100
FF3-MB	29	33
FF3-TL	57	64
FF4-OU	59	55
FF4-MB	78	91
FF4-TL	120	130
Matrix Spike	74±21.2	82±24.6

Table S6: Whole method precision (% RSD), whole method accuracy (% average recovery), method LOD, and method LOQ based on polytheylene film (sample matrix) spiked with volatile PFAS. 50 pg/μL (FTOHs, Me- and Et-FOSA, and Me- and EtFOSE) and 5 pg/μL (FTAcs and FTMAcs) volatile PFAS were spiked for whole method precision and whole method accuracy (n = 3). 0.025 – 100 pg/μL (FTOHs, Me- and Et-FOSA, and Me- and EtFOSE) and 0.0005 – 10 pg/μL (FTAcs and FTMAcs) volatile PFAS were spiked for method LOD (n = 10). Method LOQ was calculated by multiplying method LOD with 3.3.

Analyte	Whole method precision (% RSD)	Whole method accuracy (% average recovery)	Method LOD (μg/m^2)	Method LOQ (μg/m^2)
4:2 FTOH	1.0	70	2.4	8.0
6:2 FTOH	1.4	65	3.4	11
8:2 FTOH	2.2	77	8.2	27
10:2 FTOH	3.1	60	2.7	9.1
12:2 FTOH	0.90	57	3.3	11
MeFOSA	0.79	85	2.9	9.5
EtFOSA	0.52	84	3.9	13
MeFOSE	0.36	28	4.5	15
EtFOSE	4.4	33	5.1	17
4:2 FTAc	1.7	96	0.26	0.85
6:2 FTAc	1.9	117	0.21	0.70
8:2 FTAc	2.8	117	6.6	22
10:2 FTAc	3.6	133	3.1	10
6:2 FTMAc	10	101	0.23	0.78
8:2 FTMAc	16	113	0.24	0.78

Table S7: Sublayers from FF layers and amount analyzed by py-GC/MS.

FF	Layer	Sublayer	Mass sample for py-GC/MS(mg)
1	"inner" 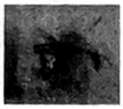	Blue yarn	128
		White yarn	83
		Yellow fabric	90
	"middle" 	Black coating	115
		White fabric	110
	"outer" 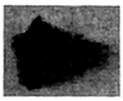	Black yarn	170
		Brown yarn	175
2	"inner" 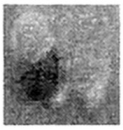	Blue yarn	123
		White yarn	79
		Yellow fabric	90
	"middle" 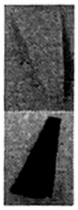	Black coating	99
		White fabric	133
	"outer" 	Brown yarn	154
		Yellow yarn	143

FF	Layer	Sublayer	Mass sample for py-GC/MS (mg)
3	"inner" 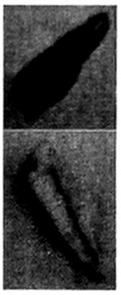	Blue yarn	172
		White yarn	61
		Yellow fabric	148
	"middle" 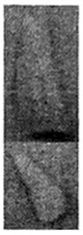	White coating	82
		White fabric	139
	"outer" 		77
4	"inner" 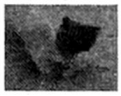	Blue yarn	90
		White yarn	76
		Yellow fabric	105
	"middle" 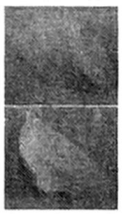	White coating	144
		White fabric	180
	"outer" 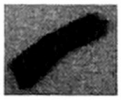	Black yarn	134
		Brown yarn	125

Table S8: Target perfluorocarboxylates (PFCA) concentrations ($\mu g/m^2$). Data for FF1-OU ($n = 4$) were provided in a

Samples	Density of Fabric ($g/4cm^2$)	PFBA	PFPeA	PFHxA	PFHpA	PFOA	PFNA	PFDA	PFUdA	PFD
FF1-OU	0.0885	2.7±3.6	0.6±0.36	1.4±0.77	1.3±1.7	0.67±1.7	1.5±1.5	0.09±0.23	<LOQ	1.1±
FF1–MB	0.0887	6.2	0.2	2.6	1.3	<LOD	0.53	0.063	<LOQ	2.(
FF1–TL	0.1446	0.43	<LOD	0.18	0.93	<LOQ	0.57	<LOD	<LOQ	<LC
FF2–OU	0.1201	2.3	0.34	1.6	1.5	0.13	0.3	0.15	0.23	0.6
FF2–MB	0.0848	5.1	0.37	2.2	1.2	<LOD	0.35	0.21	<LOQ	13
FF2–TL	0.1446	2.8	0.34	1.3	1.6	0.13	0.7	0.15	1.9	1.2
FF3–OU	0.1542	2	0.38	1.4	1.4	3.2	0.58	1.6	<LOQ	0.8
FF3–MB	0.0936	2.2	<LOD	1.6	1.1	5.6	<LOD	4.8	<LOQ	0.6
FF3–TL	0.1555	2.3	0.28	2.7	2.2	9.2	0.67	2.7	0.4	1.2
FF4–OU	0.1169	0.65	0.18	1	1.7	0.12	0.13	0.11	<LOD	<LC
FF4–MB	0.0963	1.1	<LOD	9.2	0.64	0.097	0.12	0.12	<LOQ	1.5
FF4–TL	0.1169	2	0.17	0.39	1.4	0.11	0.19	0.51	<LOQ	4.9

Table S9: Target perfluoroalkyl sulfonates (PFS) concentrations ($\mu g/m^2$). Data for FF1-OU ($n = 4$) were provided in

Samples	PFPrS	PFBS	PFPeS	PFHxS	PFHpS	PFOS	PFNS
FF1-OU	<LOD	<LOQ	<LOD	2.7±6.7	<LOD	0.65±1.6	<LOD
FF1–MB	<LOQ	4	<LOD	<LOQ	<LOD	1.2	<LOD
FF1–TL	<LOD	<LOD	<LOD	<LOQ	<LOD	<LOQ	<LOD
FF2–OU	<LOD	<LOD	<LOD	<LOQ	<LOD	0.71	<LOD
FF2–MB	<LOQ	3.5	<LOD	<LOQ	<LOD	0.59	<LOD
FF2–TL	<LOD	<LOQ	<LOD	<LOQ	<LOD	1	<LOD
FF3–OU	<LOD	<LOD	<LOD	<LOQ	<LOD	0.71	<LOD
FF3–MB	1.6	0.12	<LOD	<LOD	<LOD	0.18	<LOD
FF3–TL	<LOD	<LOD	<LOD	<LOQ	<LOD	0.56	<LOD
FF4–OU	<LOD	<LOD	<LOD	<LOD	<LOD	0.28	<LOD
FF4–MB	<LOD	<LOD	<LOD	<LOQ	<LOQ	2.1	<LOD
FF4–TL	<LOD	<LOD	<LOD	<LOQ	<LOD	0.52	<LOD

Table S10: Target Miscellaneous Electrofluorination (ECF) PFAS concentrations ($\mu g/m^2$). Data for FF1-OU ($n = 4$) deviation.

Sample	Cl-PFOS	PFEtCHxS	FBSA	FHxSA	FOSA	MeFOSA	EtFOSA	FOSAA
FF1-OU	<LOD	<LOQ	1.3±0.59	<LOD	<LOD	<LOD	<LOD	<LOD
FF1–MB	<LOD	<LOD	2.8	<LOD	<LOD	<LOD	<LOD	<LOD
FF1–TL	<LOD	<LOD	<LOD	<LOD	<LOD	<LOD	<LOD	<LOD
FF2–OU	<LOD	<LOD	<LOD	<LOD	<LOD	<LOD	<LOD	<LOD
FF2–MB	<LOD	<LOD	2	<LOD	<LOD	<LOD	<LOD	<LOD
FF2–TL	<LOD	<LOD	<LOQ	<LOD	<LOD	<LOD	<LOD	<LOD
FF3–OU	<LOD	<LOD	<LOD	<LOD	<LOD	<LOD	<LOD	<LOD
FF3–MB	<LOD	<LOD	<LOD	<LOD	<LOD	<LOD	<LOD	<LOD
FF3–TL	<LOD	<LOD	<LOD	<LOD	<LOD	<LOD	<LOD	<LOD
FF4–OU	<LOD	<LOD	<LOD	<LOD	<LOD	<LOD	<LOD	<LOD
FF4–MB	<LOD	<LOD	<LOD	<LOD	<LOD	<LOD	<LOD	<LOD
FF4–TL	<LOD	<LOD	<LOD	<LOD	<LOD	<LOD	<LOD	<LOD

Table S11: Target Miscellaneous Telomer PFAS concentrations ($\mu g/m^2$). Data for FF1-OU ($n = 4$) were provided in

Samples	4:2 FTS	6:2 FTS	8:2 FTS	10:2 FTS	3:3 FTCA	5:3 FTCA	7:3 FTCA	6:2 FTCA	8:2 FTCA	10:2 FTCA	6:2 UFTCA	8:2 UFTCA	ADONA	9 PF
FF1-OU	<LOD	8.7±21	<LOD	<LOD	<LOD	<LOD	<LOD	<LOD	<LOD	<LOD	<LOD	<LOQ	<LOD	<I
FF1–MB	<LOD	6.7	<LOD	<LOD	<LOD	16	<LOD	<LOD	<LOD	<LOD	<LOQ	<LOD	<LOD	<I
FF1–TL	<LOD	<LOD	<LOD	<LOD	<LOD	<LOD	<LOD	<LOD	<LOD	<LOD	<LOD	<LOD	<LOD	<I
FF2–OU	<LOD	0.25	<LOD	<LOD	<LOD	<LOD	<LOD	<LOD	<LOD	<LOD	<LOD	<LOD	<LOD	<I
FF2–MB	<LOD	6.3	<LOD	0.087	<LOD	23	<LOD	<LOD	<LOD	<LOD	<LOD	<LOD	<LOD	<I
FF2–TL	<LOD	<LOQ	<LOD	<LOD	<LOD	<LOD	<LOD	<LOD	<LOD	<LOD	<LOD	<LOD	<LOD	<I
FF3–OU	<LOD	<LOD	<LOD	<LOD	<LOD	<LOD	<LOD	<LOD	<LOD	<LOD	<LOD	<LOD	<LOD	<I
FF3–MB	<LOD	0.29	<LOD	<LOD	<LOD	<LOD	<LOD	<LOD	<LOD	<LOD	<LOD	<LOD	<LOD	<I
FF3–TL	<LOD	<LOD	<LOD	<LOD	<LOD	<LOD	<LOD	<LOD	<LOD	<LOD	<LOD	2.3	<LOD	<I
FF4–OU	<LOD	<LOD	<LOD	<LOD	<LOD	<LOD	<LOD	<LOD	<LOD	<LOD	<LOD	<LOD	<LOD	<I
FF4–MB	0.23	<LOQ	<LOD	<LOD	<LOD	1.2	<LOD	<LOD	<LOD	<LOD	<LOD	<LOD	<LOD	<I
FF4–TL	<LOD	<LOD	<LOD	<LOD	<LOD	<LOD	<LOD	<LOD	<LOD	<LOD	<LOD	<LOD	<LOD	<I

Table S12: Target and suspect FTOHs, Me- and Et-FOSA, and N-Methyl Perfluoroalkane Sulfonamidoethanol (Me
FF1-OU (n = 3) were provided in average±standard deviation.

Samples	4:2 FTOH	6:2 FTOH	8:2 FTOH	10:2 FTOH	12:2 FTOH	14:2 FTOH	MeFOSA	EtFOSA	MeFPrSE	MeFBSE	M
FF1-OU	<LOD	260±35	<LOD	<LOD	<LOD	<LOD	<LOD	<LOD	<LOD	<LOQ	·
FF1–MB	<LOD	160	<LOD	<LOD	<LOD	<LOD	<LOD	<LOD	<LOD	9300	·
FF1–TL	<LOD	<LOD	<LOD	<LOD	<LOD	<LOD	<LOD	<LOD	<LOD	<LOQ	·
FF2–OU	<LOD	79	<LOD	<LOD	<LOD	<LOD	<LOD	<LOD	<LOD	<LOQ	·
FF2–MB	<LOD	170	<LOD	<LOD	<LOD	<LOD	<LOD	<LOD	<LOD	8400	·
FF2–TL	<LOD	190	<LOD	<LOD	<LOD	<LOD	<LOD	<LOD	<LOD	<LOQ	·
FF3–OU	<LOD	<LOD	110	32	<LOD	<LOD	<LOD	<LOD	<LOD	<LOQ	·
FF3–MB	<LOD	<LOD	460	270	89	<LOD	<LOD	<LOD	<LOD	<LOQ	·
FF3–TL	<LOD	<LOD	<LOD	8.7	<LOD	<LOD	<LOD	<LOD	<LOD	<LOQ	·
FF4–OU	<LOD	3500	<LOD	<LOD	<LOD	<LOD	<LOD	<LOD	<LOD	<LOQ	·
FF4–MB	<LOD	140	<LOD	<LOD	<LOD	<LOD	<LOD	<LOD	<LOD	<LOQ	·
FF4–TL	<LOD	19	<LOD	<LOD	<LOD	<LOD	<LOD	<LOD	<LOD	<LOQ	·

Table S13: Target and suspect N-Ethyl Perfluoroalkane Sulfonamidoethanol (EtFASEs), FTAcs, and FTMAcs conc (n = 3) were provided in average±standard deviation. FTIs, PFIs, or FTOs were <LOD for all samples.

Samples	EtFEtSE	EtFPrSE	EtFBSE	EtFPeSE	EtFHxSE	EtFHpSE	EtFOSE	4:2 FTAc	6:2 FTAc	
FF1-OU	<LOQ	<LOD	<LOD	<LOD	<LOD	<LOD	<LOQ	<LOD	<LOD	<
FF1–MB	<LOQ	<LOD	<LOD	<LOD	<LOD	<LOD	<LOQ	<LOD	<LOD	<
FF1–TL	<LOD	<LOD	<LOD	<LOD	<LOD	<LOD	<LOQ	<LOD	<LOD	<
FF2–OU	<LOD	<LOD	<LOD	<LOD	<LOD	<LOD	<LOQ	<LOD	<LOD	<
FF2–MB	<LOD	<LOD	<LOD	<LOD	<LOD	<LOD	<LOQ	<LOD	<LOD	<
FF2–TL	<LOD	<LOD	<LOD	<LOD	<LOD	<LOD	<LOQ	<LOD	<LOD	<
FF3–OU	<LOQ	<LOD	<LOD	<LOD	<LOD	<LOD	270	<LOD	<LOD	
FF3–MB	<LOQ	<LOD	<LOD	<LOD	<LOD	<LOD	80	<LOD	<LOD	
FF3–TL	<LOQ	<LOD	<LOD	<LOD	<LOD	<LOD	80	<LOD	<LOD	
FF4–OU	<LOQ	<LOD	<LOD	<LOD	<LOD	<LOD	<LOQ	<LOD	<LOD	
FF4–MB	<LOQ	<LOD	<LOD	<LOD	<LOD	<LOD	<LOQ	<LOD	<LOD	
FF4–TL	<LOD	<LOD	<LOD	<LOD	<LOD	<LOD	<LOQ	<LOD	<LOD	

Table S14: Total fluorine concentrations by PIGE and INAA. FF3 was manufactured in 2008 while FF1, 2, and 4 were manufactured in 2019.

Firefighter Turnout Suit #	PIGE (mg F/kg)	INAA (mg F/kg)
FF1-TL	18	<LOD
FF1-MB	Off scale	122,000
FF1-O	5,960	4,950
FF2-TL	2,030	1,430
FF2-MB	Off scale	120,000
FF2-O	4,110	2,650
FF3-TL	32	13
FF3-MB	Off scale	116,000
FF3-O	2,540	2,360
FF4-TL	17	< LOD
FF4-MB	Off scale	43,700
FF4-O	6,250	5,480

< LOD = less than the limit of detection; off-scope indicates signal off the upper end of the PIGE calibration range (100,000 mg F/kg)

Figure S1: Workflow schematic for comparison by spectral contrast angles of py-GC/MS Analysis

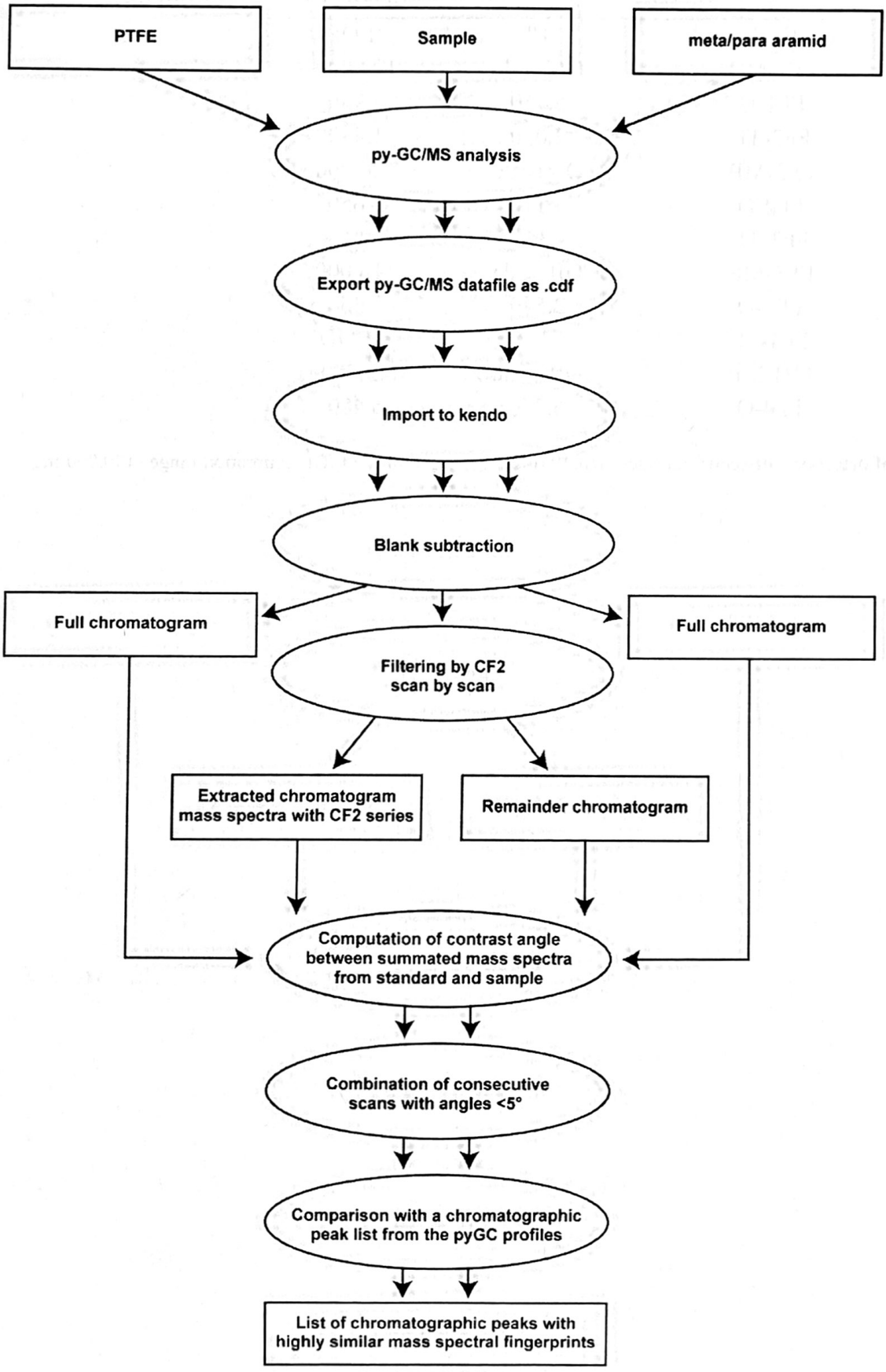

Figure S2: Frequency of Detection for Non-volatile and Volatile PFAS in all firefighter turnout gear pants.

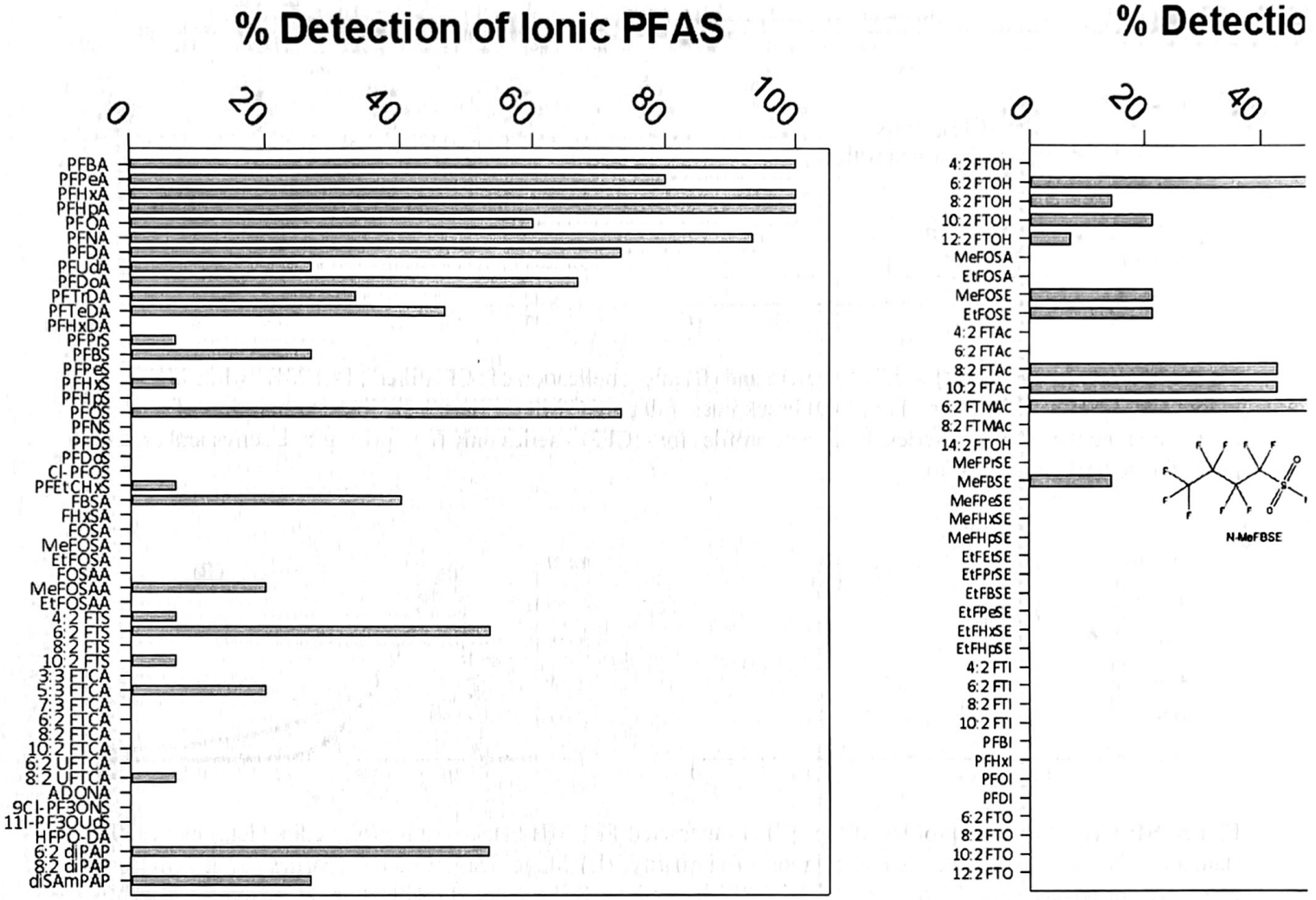

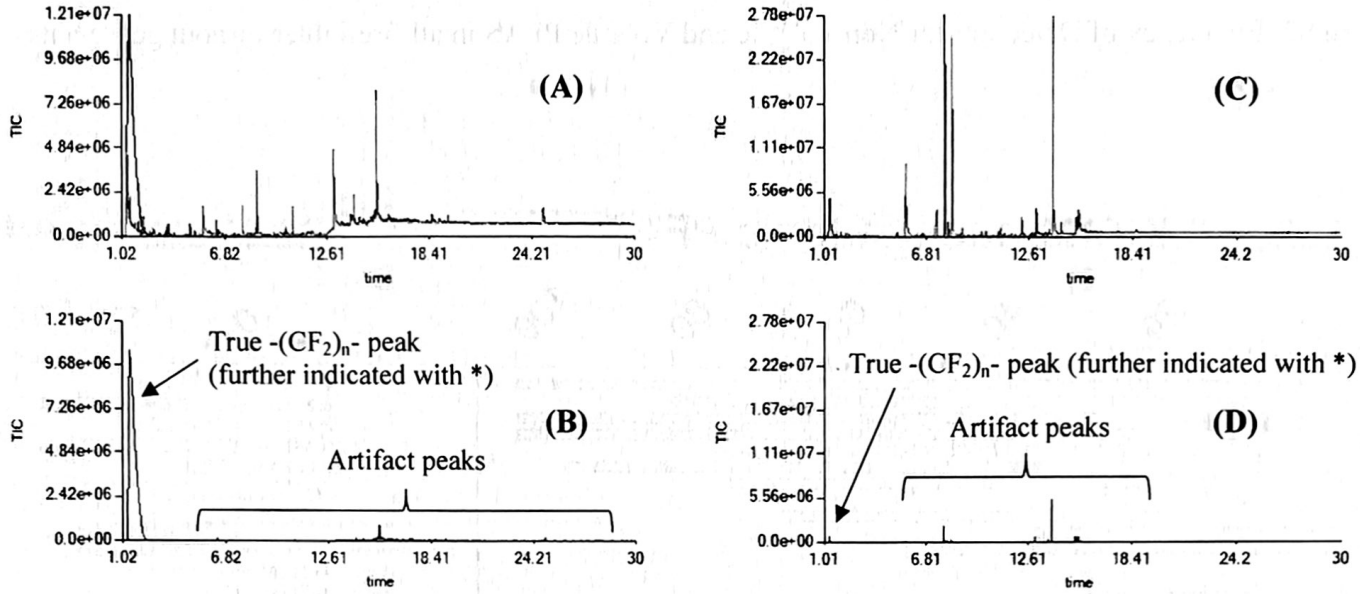

Figure S3: TIC for FF1 MB "black" (A) before and (B) after application of "CF_2-filter". FF1 MB "white" (C) before and (D) after "CF_2-filter". For (A-D) Black lines: full py-GC/MS profiles; Blue lines: remainders of profiles after extracting the $-(CF_2)_n-$ series; Red lines: profiles for $-(CF2)_n-$ series only (comprising true series and artifact peaks due to background noise).

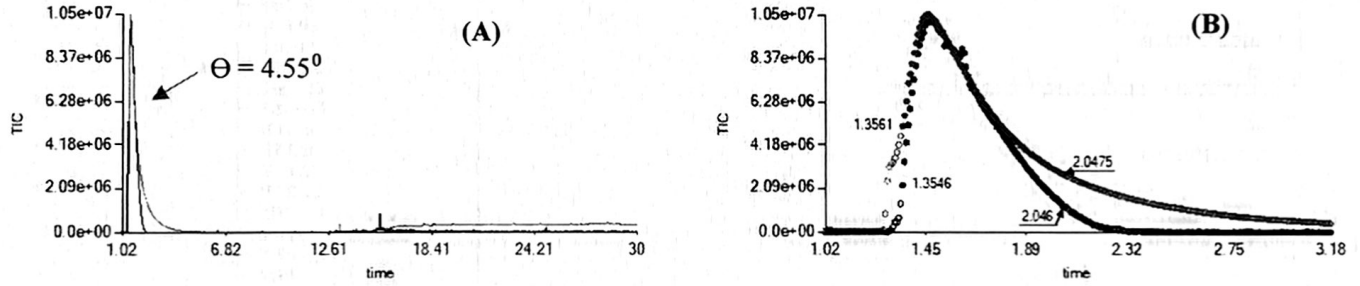

Figure S4: (A) Py-GC/MS profiles of the $-(CF_2)_n-$ extracted FF1 MB black coating (black line/dots) and a PTFE standard (blue line/dots) with the computation of similarity. (B) Magnification of the profiles. Theta angles are computed for concatenated scans within a +/- 0.015 min width. If the spectral-contrast-angle between consecutive summed mass spectra from concatenated scan from the sample and the standard is $<5^0$, the concatenated scans are combined. Filled dots = combined scans with Θ angles $<5^0$deg (average Θ for 1.35-2.05 min: 4.55 deg)

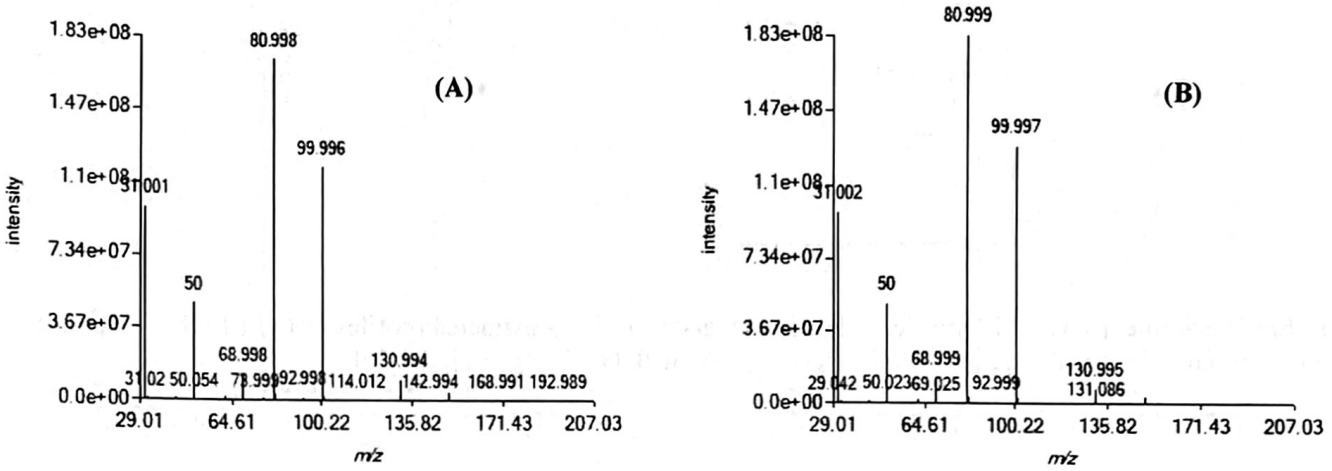

Figure S5: (A) Mass spectrum from the -$(CF_2)_n$- extracted FF1 MB black coating py-GC/MS profile with theta <5 deg vs PTFE (filled black dots, 1.35-2.05 min) (B) Mass spectrum from the raw PTFE py-GC/MS profile with theta <5 deg vs –$(CF2)_n$- extracted FF1 "middle" black coating (filled blue dots, 1.35-2.05 min)

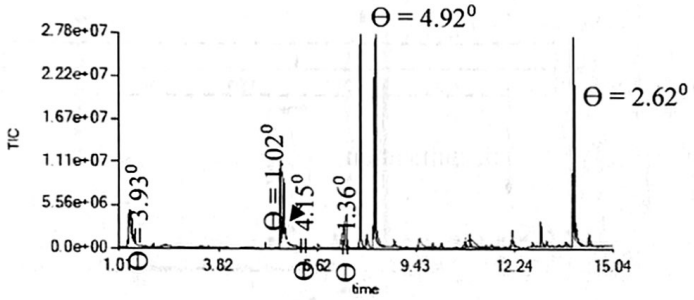

Figure S6: Black line: py-GC/MS profile or the remainders of -$(CF_2)_n$- extracted profiles from FF1 MB white fabric Blue line: py-GC/MS profile of meta-aramid. Py-GC peaks with Θ <5°deg are indicated.

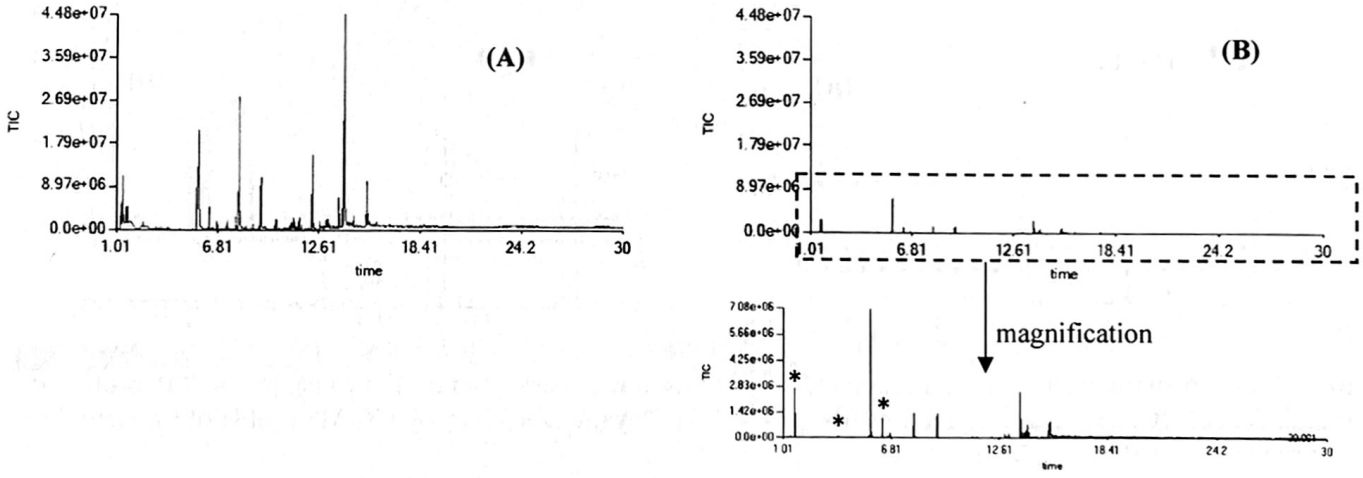

Figure S7: (A) Py-GC/MS profile of FF1 OU black yarn (black line) and remainder of CF_2-extraction profile (blue line) (B) CF2-extracted profile of FF1 OU black yarn (red line)

Θ = 2.5°

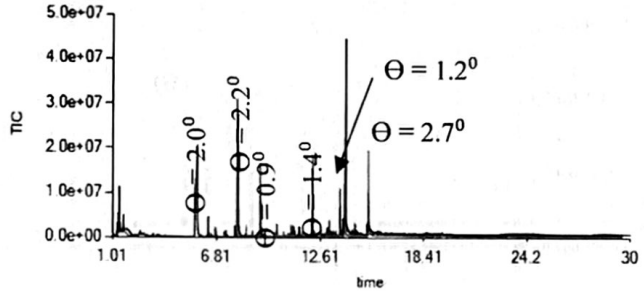

Figure S8: Black line: py-GC/MS profile or the remainders of -$(CF2)_n$- extracted profiles from FF1 OU black yarn Blue line: py-GC/MS profile of para-aramid. Py-GC peaks with Θ <5⁰deg are indicated.

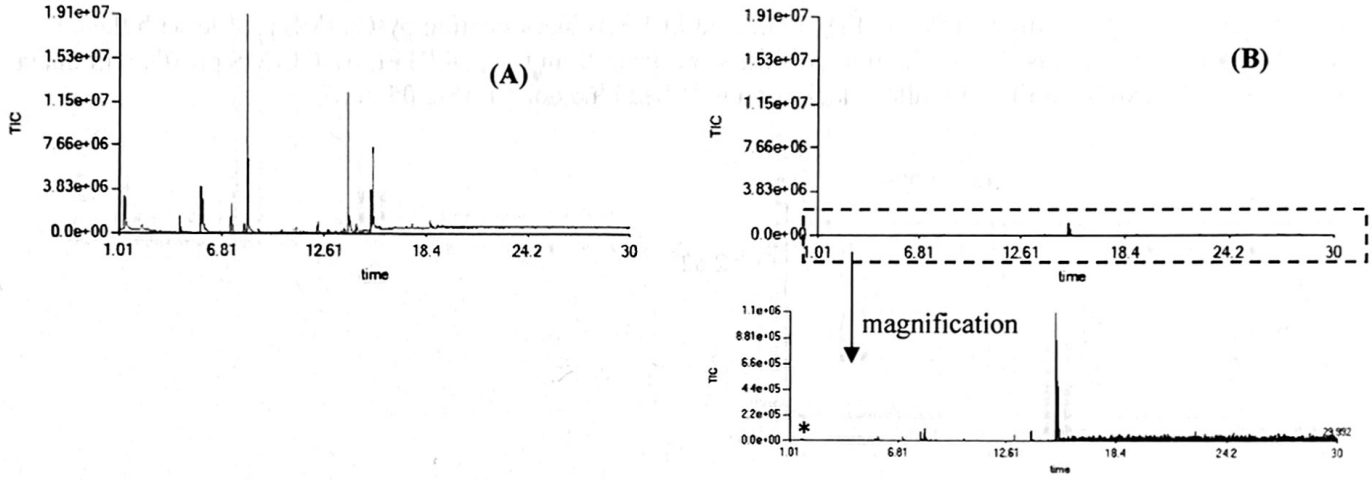

Figure S9: (A) Py-GC/MS profile of FF1 TL white yarn (black line) and remainder of CF_2-extraction profile (blue line) (B) CF2-extracted profile of FF1 TL white yarn (red line)

(A) Comparison with meta-aramid

(B) Comparison with para-aramid

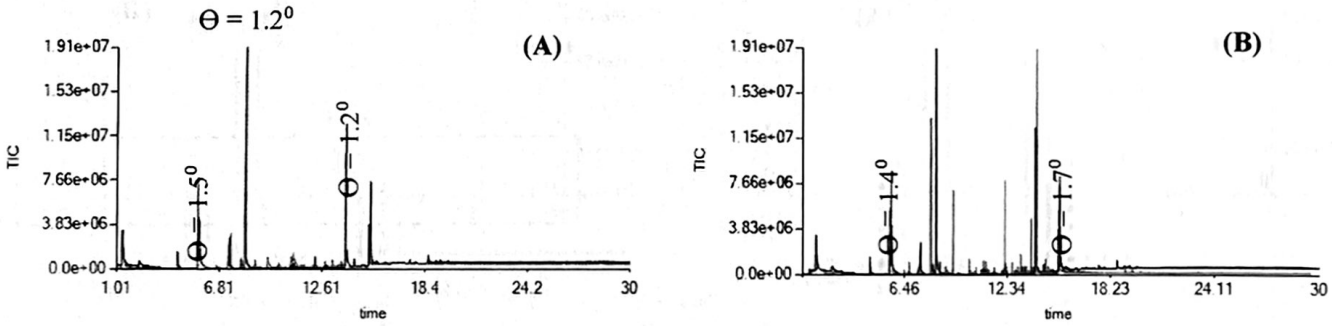

Figure S10: (A) Comparison with meta-aramid (B) Comparison with para-aramid. Black line: py-GC/MS profile or the remainders of -$(CF2)_n$- extracted profiles from FF1 TL black yarn. Blue line: py-GC/MS profile of standard. Py-GC peaks with Θ <5⁰deg are indicated.

Equations

Theoretical PTFE film Concentration

$$1\ kg\ PTFE \times \frac{1000\ g\ [CF_2CF_2]}{1\ kg\ PTFE} \times \frac{1\ mole\ [CF_2CF_2]}{99.9936\ g} \times \frac{4\ moles\ F}{1\ M\ [CF_2CF_2]} \times \frac{18.9984\ g}{1\ mole\ F} = \frac{760\ g\ F}{1\ kg\ PTFE} \quad \textbf{Eq S1}$$
$$= 760{,}000\ ppm\ F$$

Fraction of PTFE film on MB layer

$$[Fraction\ due\ to\ PTFE\ layer]\ kg\ [Theoretical\ PTFE\ Film\ concentration] + ([Fraction\ due\ to\ non-PTFE\ layer]kg)[Concentration\ of\ non-PTFE\ layers]\ (See\ -OU\ example] = [Measured\ total\ F\ Concentration] \quad \textbf{Eq S2}$$

$$[X]\ kg\left[760{,}000\ mg\frac{F}{kg}\right] + (1\ kg - [X]kg)[5{,}000\ mg\ F/kg]\ (See\ FFX-OU\ example] = [122{,}000\ mg\ F/$$

$$[X]\ kg\left[760{,}000\ mg\frac{F}{kg}\right] + (5{,}000\ mg\ F/kg - [X][5{,}000\ mg\ F/kg]) = [122{,}000\ mg\ F/kg]$$

$$[X]\ kg\left[760{,}000\ mg\frac{F}{kg}\right] - [X][5{,}000\ mg\ F/kg] = [122{,}000\ mg\ F/kg] - [5{,}000\ mg\ F/kg]$$

$$[X]kg\left[755{,}000\ mg\frac{f}{kg}\right] = 117{,}000\ mg\frac{F}{kg}$$

$$[X] = 0.155\ \times 100\% = 15.5\%$$

Total weight percent of F on non-PTFE layer

$$\frac{5{,}000\ mg\ F}{kg} \times \frac{1\ kg\ Fiber}{1000\ g\ Fiber} = 5\frac{mg\ F}{g}\ Fiber = \frac{5\ mg\ F}{1000\ mg\ Fiber} \times 100\% = 0.5\ wt\ \%\ F \quad \textbf{Eq S3}$$

Conversion from μg/m² to ng/g

$$\frac{\mu g}{m^2} \times \frac{1\ m^2}{10{,}000\ cm^2} \times \frac{1000\ ng}{1\ \mu g} \times Density\ of\ Fabric^{-1}\left(\frac{cm^2}{g}\right) = \frac{ng}{g} \quad \textbf{Eq S4}$$

References

1. Robel, A. E.; Marshall, K.; Dickinson, M.; Lunderberg, D.; Butt, C.; Peaslee, G.; Stapleton, H. M.; Field, J. A., Closing the Mass Balance on Fluorine on Papers and Textiles. *Environ. Sci. Technol.* **2017,** *51*, (16), 9022-9032.
2. Backe, W. J.; Day, T. C.; Field, J. A., Zwitterionic, cationic, and anionic fluorinated chemicals in aqueous film forming foam formulations and groundwater from us military bases by nonaqueous large-volume injection HPLC-MS/MS. *Environ. Sci. Technol.* **2013,** *47*, (10), 5226-5234.
3. Vial, J.; Jardy, A., Experimental comparison of the different approaches to estimate LOD and LOQ of an HPLC method. *Anal. Chem.* **1999,** *71*, (14), 2672-2677.
4. Rewerts, J. N.; Morre, J. T.; Simonich, S. L. M.; Field, J. A., In-Vial Extraction Large Volume Gas Chromatography Mass Spectrometry for Analysis of Volatile PFASs on Papers and Textiles. *Environ. Sci. Technol.* **2018,** *52*, (18), 10609-10616.
5. Rodowa, A. E.; Christie, E.; Sedlak, J.; Peaslee, G. F.; Bogdan, D.; DiGuiseppi, B.; Field, J. A., Field Sampling Materials Unlikely Source of Contamination for Perfluoroalkyl and Polyfluoroalkyl Substances in Field Samples. *Environ. Sci. Technol. Lett.* **2020,** *7*, (3), 156-163.
6. Wan, K. X.; Vidavsky, I.; Gross, M. L., Comparing similar spectra: From similarity index to spectral contrast angle. *J. Am. Soc. Mass Spectrom.* **2002,** *13*, (1), 85-88.
7. Dolan, M. J.; Blackledge, R. D.; Jorabchi, K., Classifying single fibers based on fluorinated surface treatments. *Anal. Bioanal. Chem.* **2019,** *411*, (19), 4775-4784.
8. Peaslee, G. F.; Wilkinson, J. T.; McGuinness, S. R.; Tighe, M.; Caterisano, N.; Lee, S.; Gonzales, A.; Roddy, M.; Mills, S.; Mitchell, K., Another Pathway for Firefighter Exposure to Per- and Polyfluoroalkyl Substances: Firefighter Textiles. *Environ. Sci. Technol. Lett.* **2020,** *7*, (8), 594-599.